

Muon Microscopes

Yukinori NAGATANI
(KEK IMSS)

Contents

1. $T\mu M$:

Transmission Muon Microscopy

2. $S\mu^+ M$:

Scanning positive Muon Microscopy

3. $S\mu^- M$:

Scanning negative Muon Microscopy

T μ M: **Transmission Muon Microscopy**

It visualizes Electromagnetic Fields
in thick specimen

Our Goals by Visualizing Ele/Mag-field

- **Our modern civilization is constructed on Electromagnetism.**
Computer / Semiconductor / Communication dev. / EV / Rader / ...

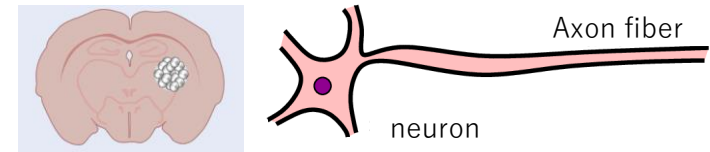
- **Power Devices: Power/RF Tr, Capacitor, Magnet, Battery, Piezo, ...**



Making them **higher voltage / higher speed / higher efficiency** contributes to **industrial benefits** and **SDGs** of our society by realizing smarter EV / power grid / comm. networks / radar ...

- **Visualization of EM-field** in devices makes them higher performance.
eg. : Specifying field concentration \leftrightarrow design of relaxation \rightarrow Higher voltage dev.

- **Brain / Nerves system uses network of action potential to process our thinking, emotion or consciousness**



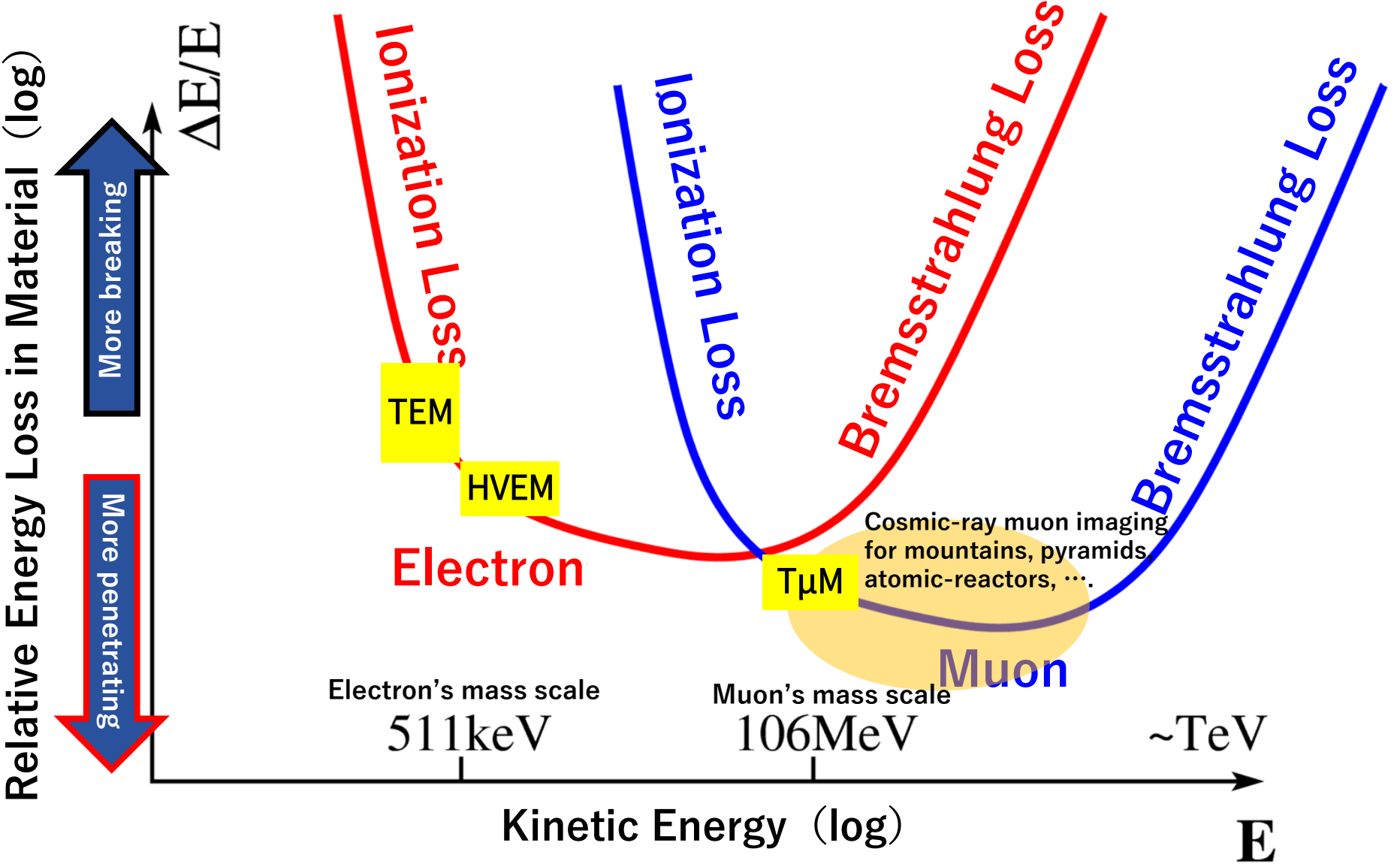
Visualization of EM-field in bulk object is quite important subject in wide fields including industry and life science.

Muon can visualize EM-fields in objects

- Muon is **charged particle** → **Sensitivity both E and B field**
- **The highest material permeability** by acceleration
- **Mass production** by accelerator
- **High resolution** and **high sensitivity** by beam-cooling
- **Magnification of Image / Visualization of EM field**
by Electron Microscopy Technologies
- **High resolutional Image-detection** by Direct-detecting CMOS
Image Sensors for Electron Microscopy

**Combining accelerator technology and
electron microscopy one allows us it**

Penetration-capability of e and μ



Transmission Electron Microscopy (TEM)

It visualizes EM-field by highest resolution:

Methods : Lorentz Microscopy, Electron Holography, Phase-Contrast TEM

Targets : Transistor(Rau), Mag-field among atoms(Shibata),

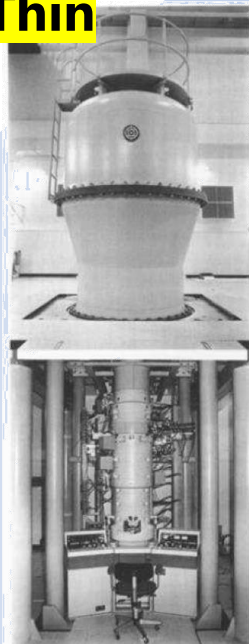
Membrane Potential for liposome (Sigworth), ...

Specimen should be **Ultra-Thin**

(depending on beam energy)



200 kV cryo-TEM



1 MV HVEM @ NIPS



World Highest
3 MV HVEM @ Osaka U.

Observable
Thickness

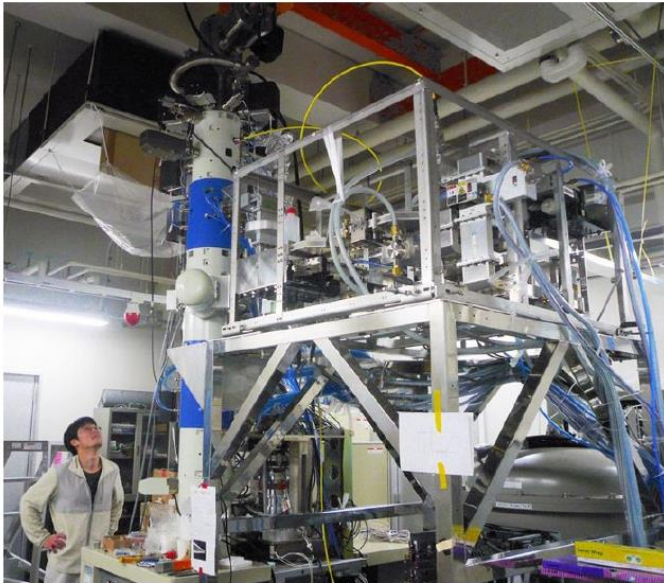
~200 nm

~ 1 μ m

~ 3 μ m

Recent Topics : HVEM by RF-Accelerators

Recently, linear accelerators are applied into HV-TEMs.



This high-voltage transmission electron microscope is much smaller than earlier models, which can take up an entire two-storey building. Credit: Yukinori Nagatani/NIPS

PHYSICS · 18 OCTOBER 2019

How to improve a huge super-resolution microscope: shrink it

Physicists redesign an enormous and costly imaging device to make it smaller and cheaper.

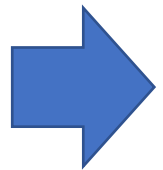


NIPS 500kV Linac TEM
by Y.N. [PRL123(15)2019]

Osaka U. 3MV RF-Gun TEM
by J. Yang [Microscopy, 291-295 (2018)]

Concept of Transmission Muon Microscopy (T μ M)

- Properties of electron and muon are very similar.
- Accelerator-generated muon can be higher luminance.
- Accelerated muon has strong penetration capability to materials



By employing muons instead of electrons in TEM, Ele/Mag-fields in thick object are visualized.

Essence of the Transmission Muon Microscopy (T μ M)

Comparing with present methods

	Mag-field	Ele-field	Penetration Power	Versatility of specimen
muon (T μ M)	○	○	○ 10 μ m ~ cm	Widely acceptable
electron (TEM)	○	○	× 100s nm ~ a few μ m	should be Ultra-thin
neutron	○	×	○ a few cm	Widely acceptable except for B, Gd, Cd, ...
Circular polarized X-ray	$\triangle_{\text{indirect}}$	×	\triangle 10 μ m	should has X-ray magnetic circular dichroism.
Optical Kerr scope	$\triangle_{\text{indirect}}$	$\triangle_{\text{indirect}}$	transparent or surface	Limited to transparent magnetic or nonlinear optical materials.
Ca-Imaging fluorescence microscope	×	$\triangle_{\text{indirect}}$	transparent life-tissue	Ca density measurement in life.

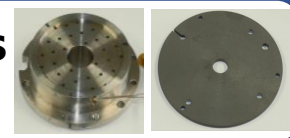
Phase 1: 5MeV TμM

Muon Beam Cooling

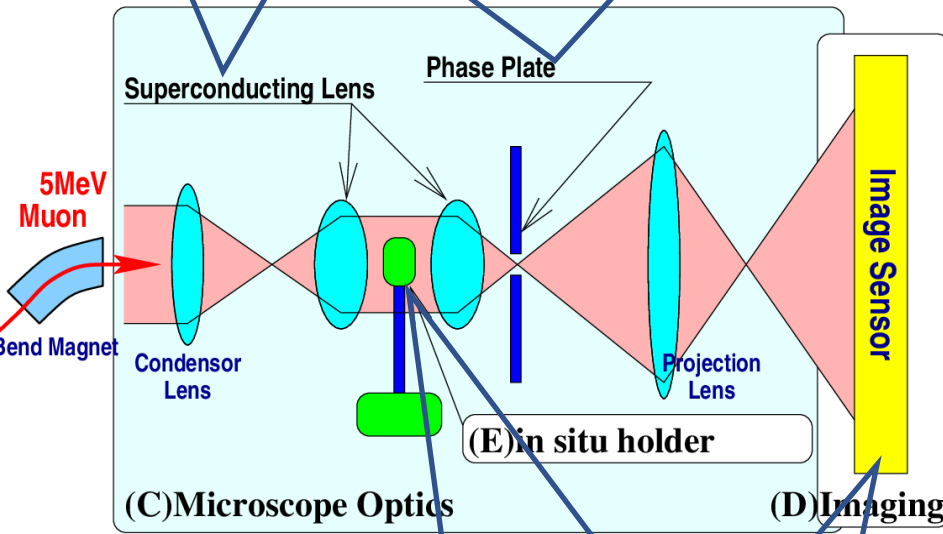
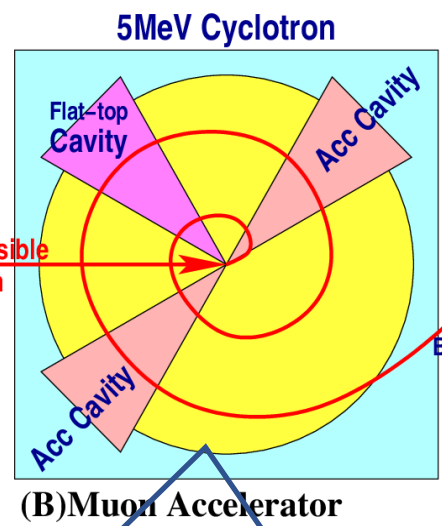
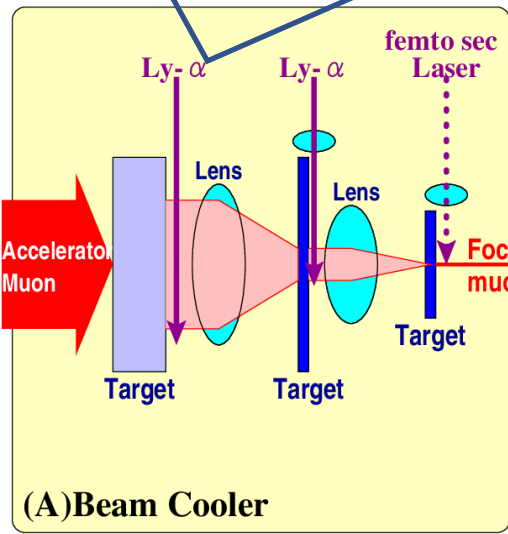
- 4-step cooling system is planned
- The first step has been already working
- The steps are increased step by step
- The final step uses femto-sec laser

Superconducting Object Lens

focuses accelerated μ-beam

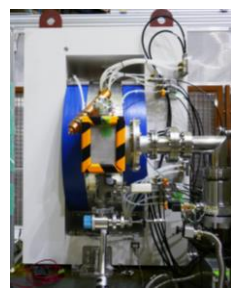


Lorentz / Phase-contrast optics for muon



5 MeV Muon Cyclotron

- AVF-type, Flat-top RF accel.
- $\Delta E / E \sim 10^{-5}$ (goal)
- Time to accel. < 1 μsec
- Already been installed at MLF!



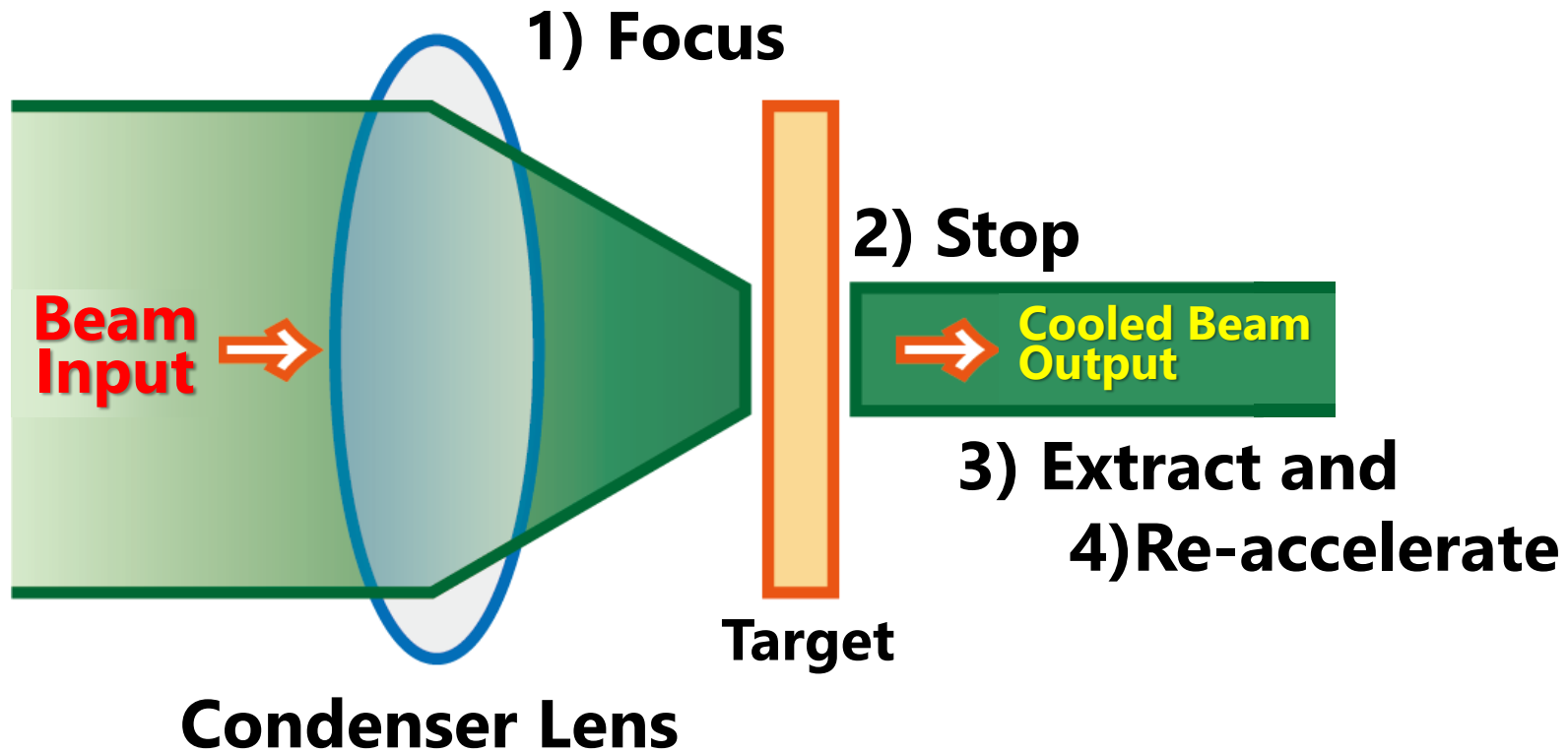
In situ specimen holder for Power-device / Life

CMOS Image Sensor for TEM is employed



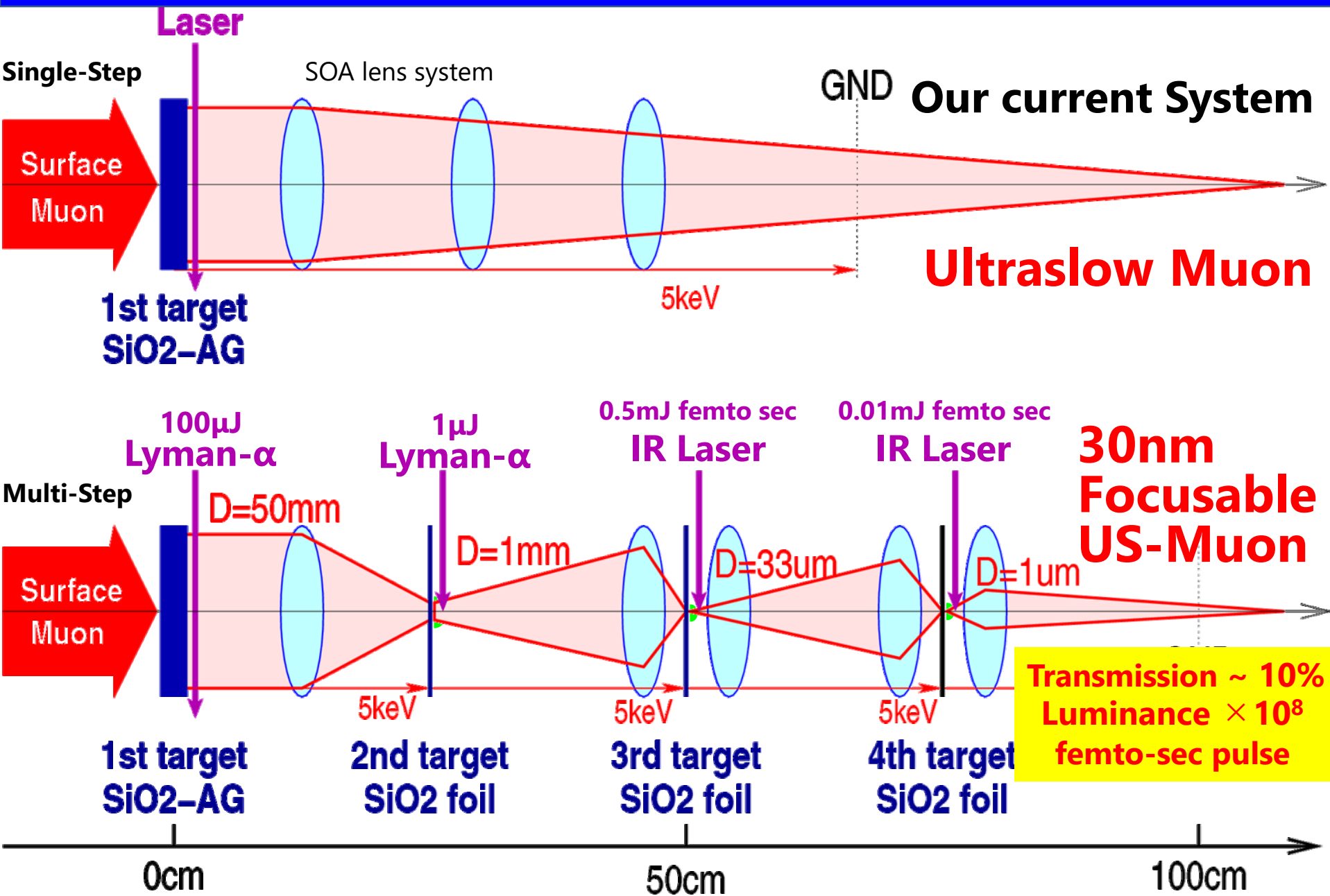
Digital Camera Sensor has been checked. 10

Essence of the Beam Cooling



- Momentum distribution is cleared by stopping.
- Volume in phase space (emittance) is shrunken down. = Beam-Cooling
- Iteration of this process can cool the beam down much more.

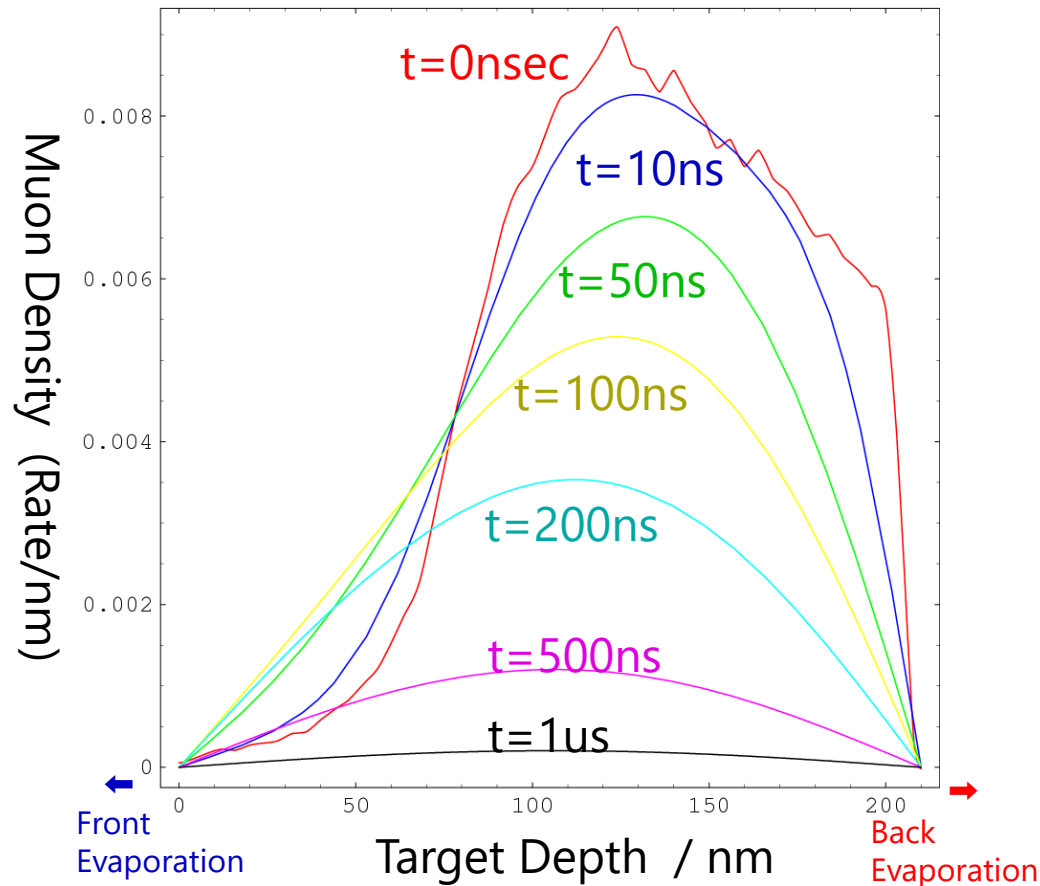
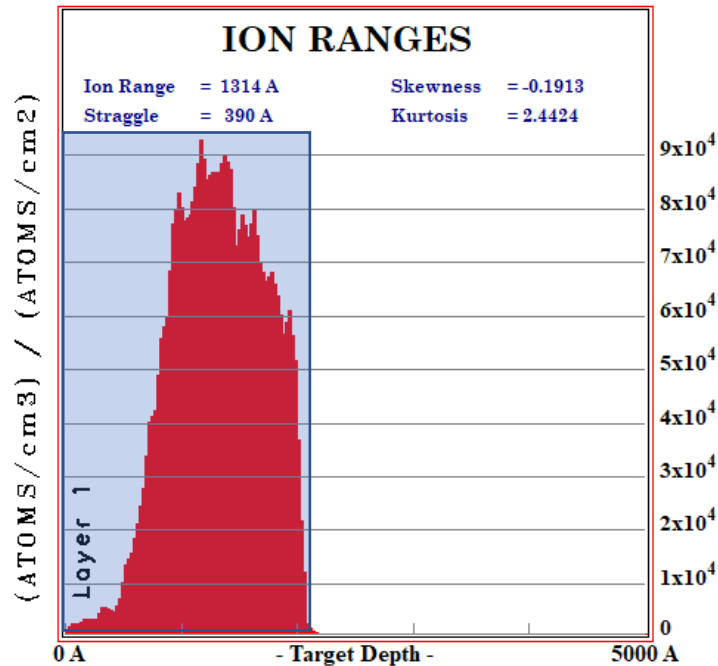
Single-step / Multi-step Beam Cooling



Diffusion in the thin target

Diffusions of Mu in mesoporous silica are evaluated

$t=210\text{nm}$, $\rho = 1.1\text{g/cm}^3$, $D=1.6 \times 10^{-4}\text{cm}^2/\text{sec} = 16 \text{ nm}^2/\text{nsec}$.



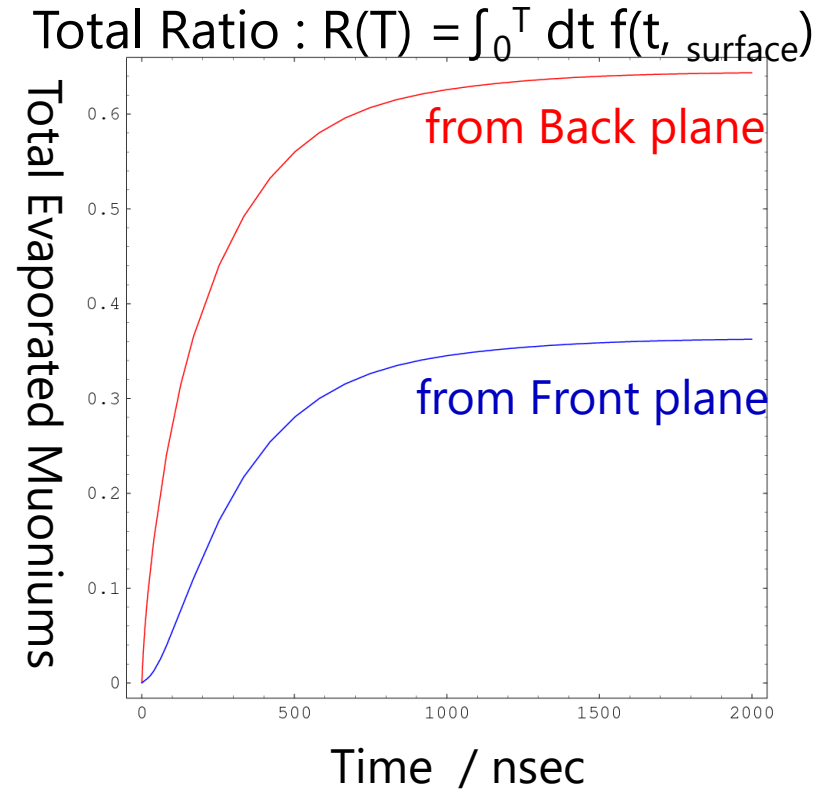
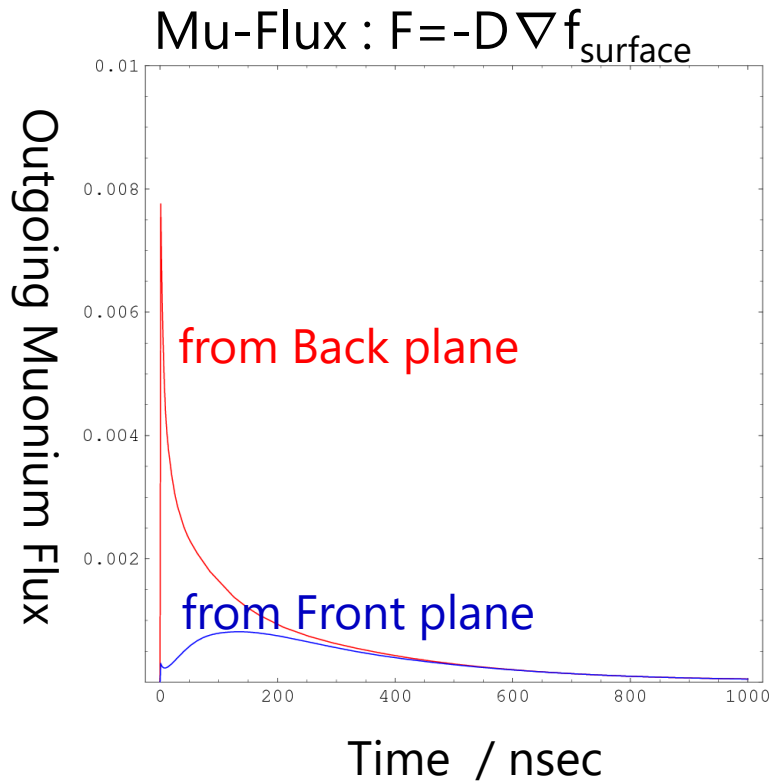
SRIM Simulation

➔ Diffusion Equation Analysis

Mu-distribution : $f(t,x)$,

Eq: $df/dt = D \Delta f$, BC: $f(t, \text{surface}) = 0$, $f(0,x) = \{\text{SRIM-Result}\}$.

Mu-Evaporation from the target



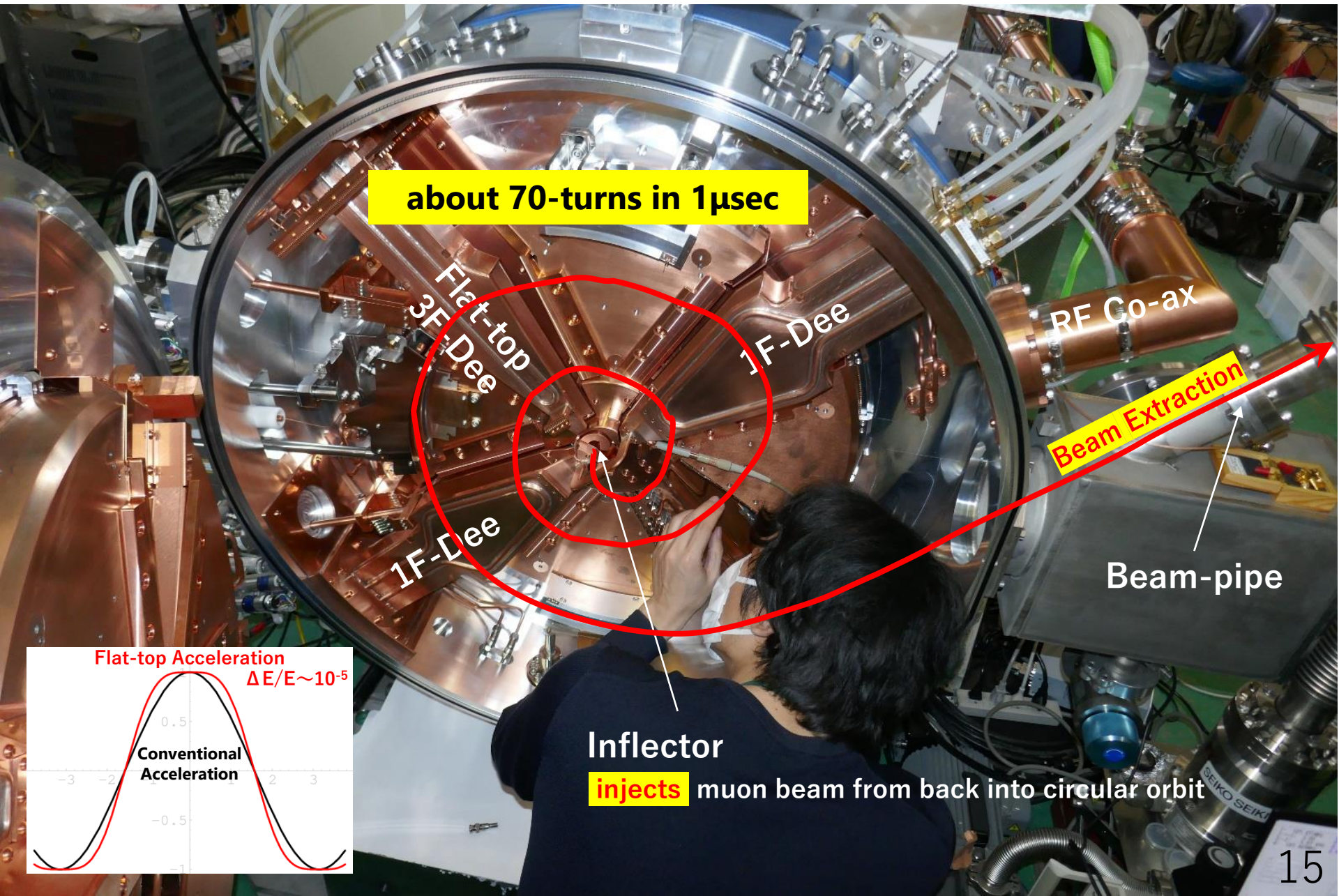
Muoniums are evaporated

~60% from back plane and ~30% from front plane.

Rate for passing thorough additional 3steps $\sim > 10\%$.

The 3 steps-cooler improves $\times 10^8$ Luminance for US-Muon beam.

5MeV Muon Cyclotron



about 70-turns in 1 μ sec

Flat-top
3F-Dee

1F-Dee

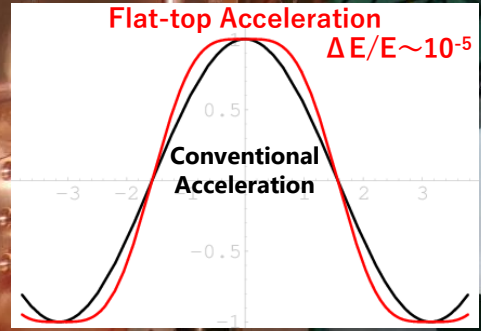
RF Co-ax

Beam Extraction

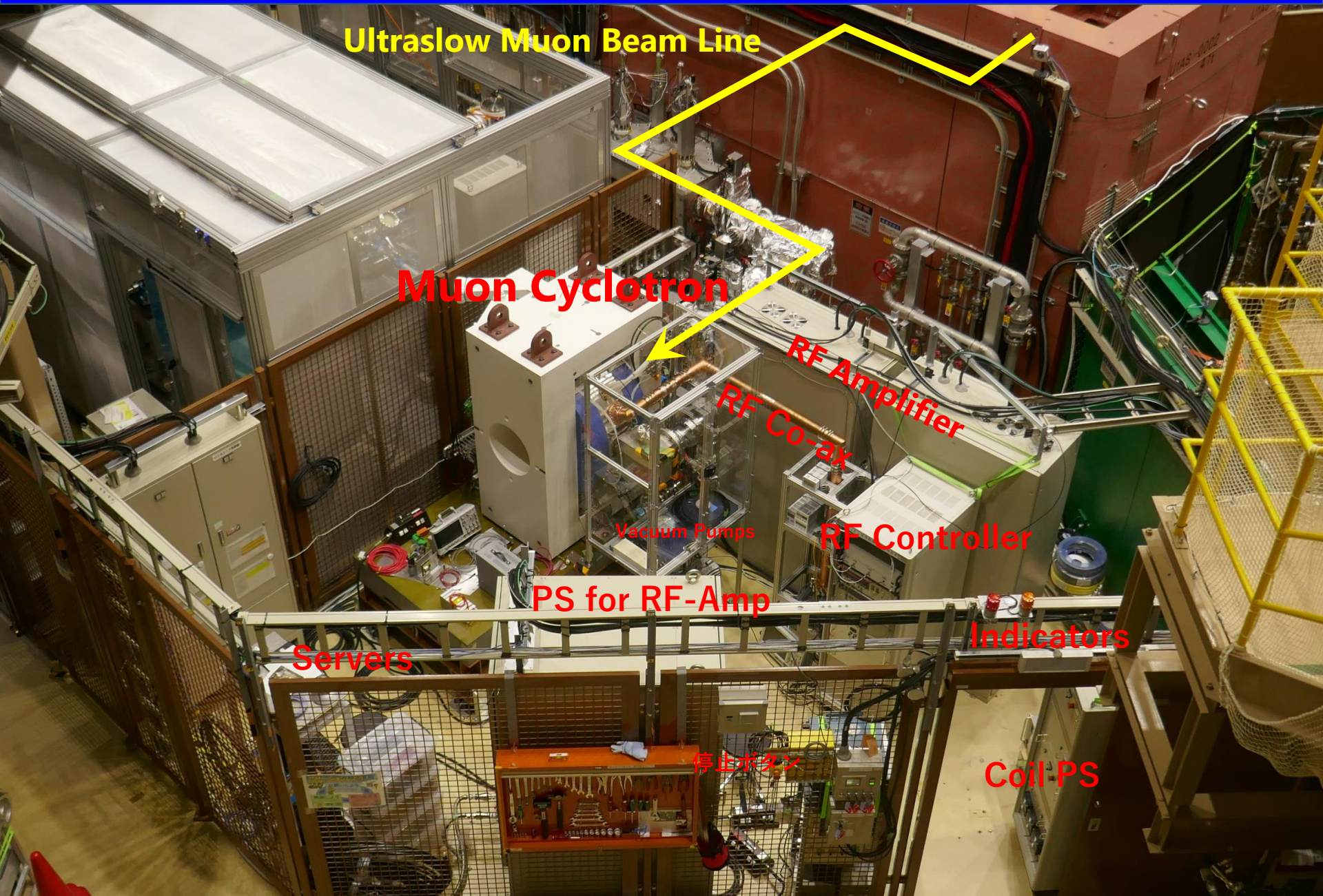
Beam-pipe

Inflector

injects muon beam from back into circular orbit



Cyclotron installed in U1B area MFL/J-PARC



Ultralow Muon Beam Line

Muon Cyclotron

RF Amplifier

RF Co-ax

Vacuum Pumps

RF Controller

PS for RF-Amp

Servers

Indicators

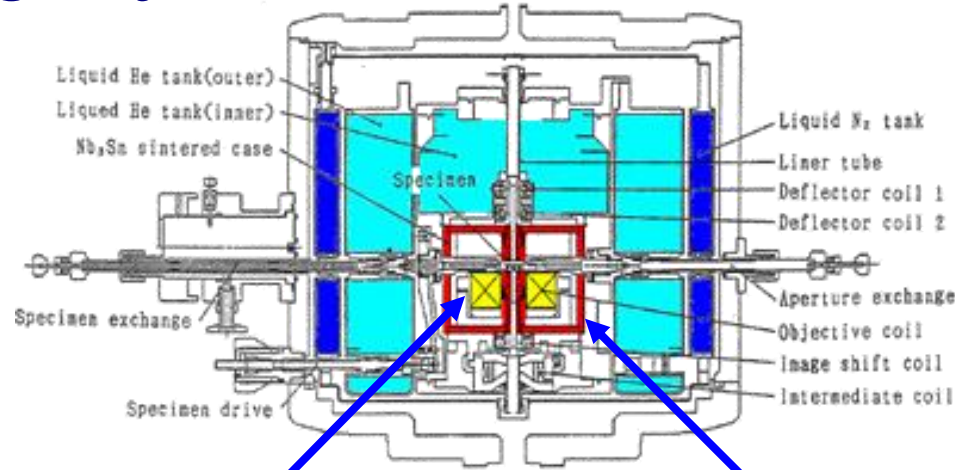
停止ボタン

Coil PS

R&D of lenses for T μ M

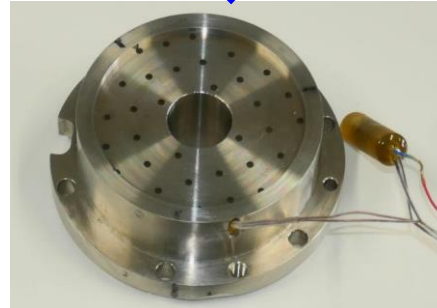
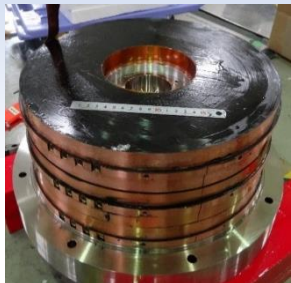
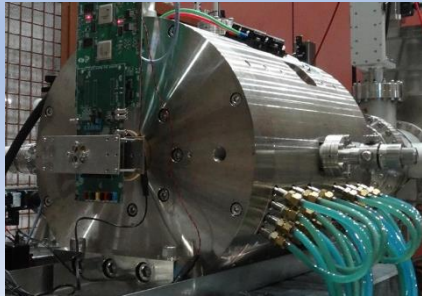
Superconducting Object Lens

Developed by I. Dietrich

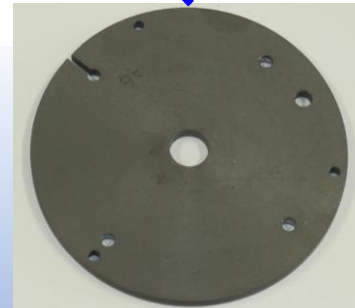


Transfer from
JEOL to KEK

Normal Conductor Lens

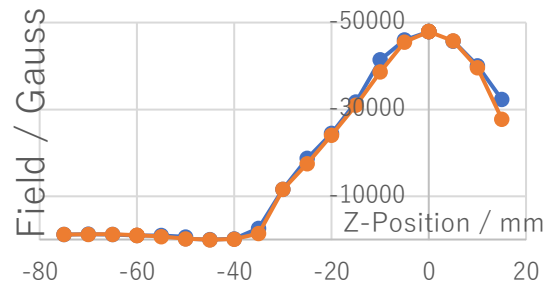


Superconducting Coil
with persistent current SW



Meissner Shield
for field convergence

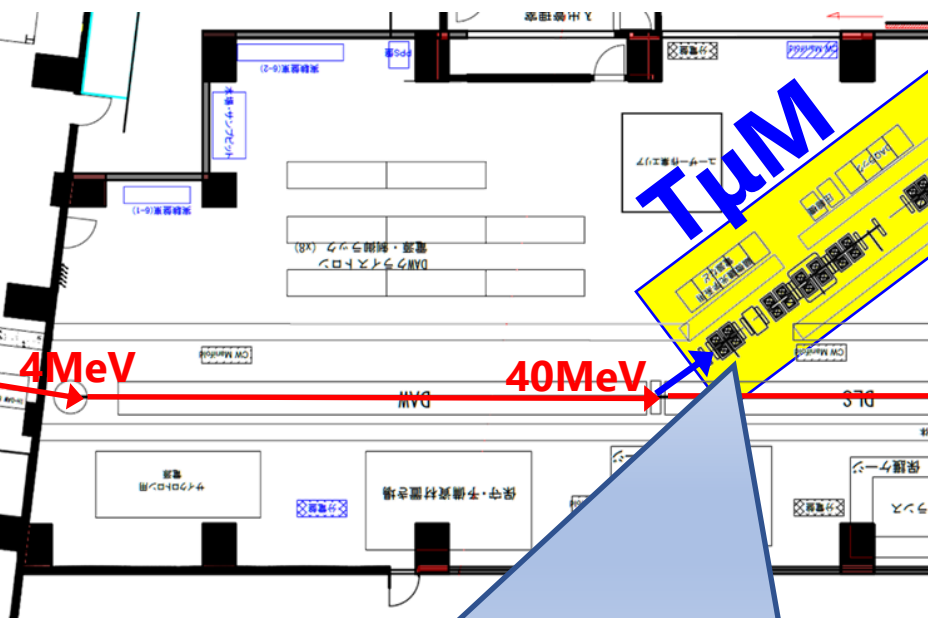
Magnetic field is
guided to be focused
by Meissner shields
rather than pole-piece
/ yoke.



**40MeV T μ M becomes
8~9m Length by
scaling design of TEMs.**

Phase 2: 40MeV T μ M

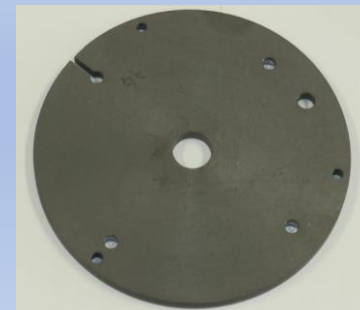
At the H2 extension building, max synergy with the g-2/EDM experiment



Superconducting Lenses are employed



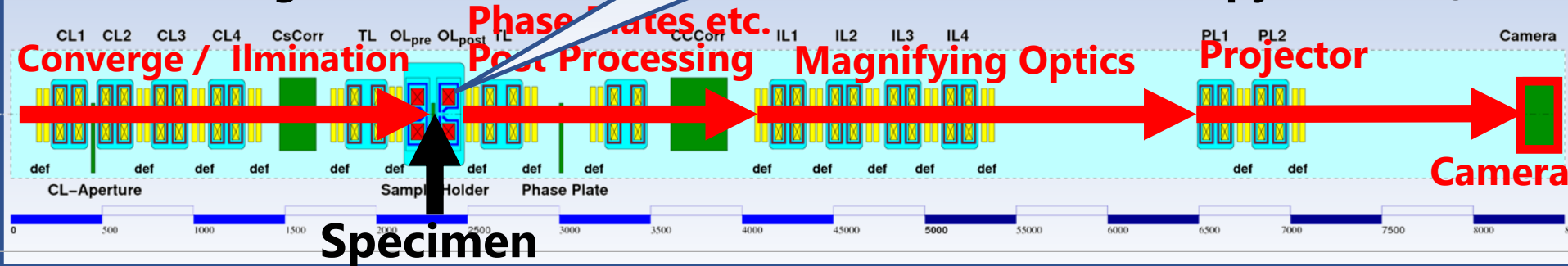
Superconducting Coil
with persistent current SW



Meissner Shield
for field convergence

Magnetic field is guided to be focused by Meissner shields rather than pole-piece / yoke.

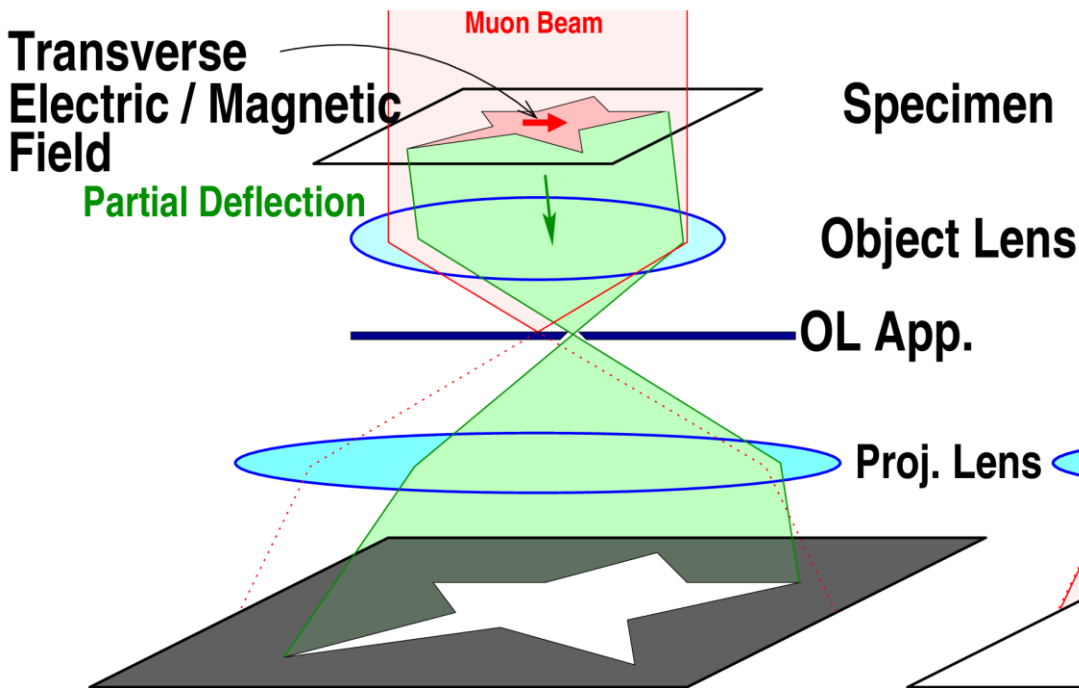
Column Design of the 40MeV Transmission Muon Microscopy $\sim 9\text{m}$ length



Visualization of Electromagnetic Fields

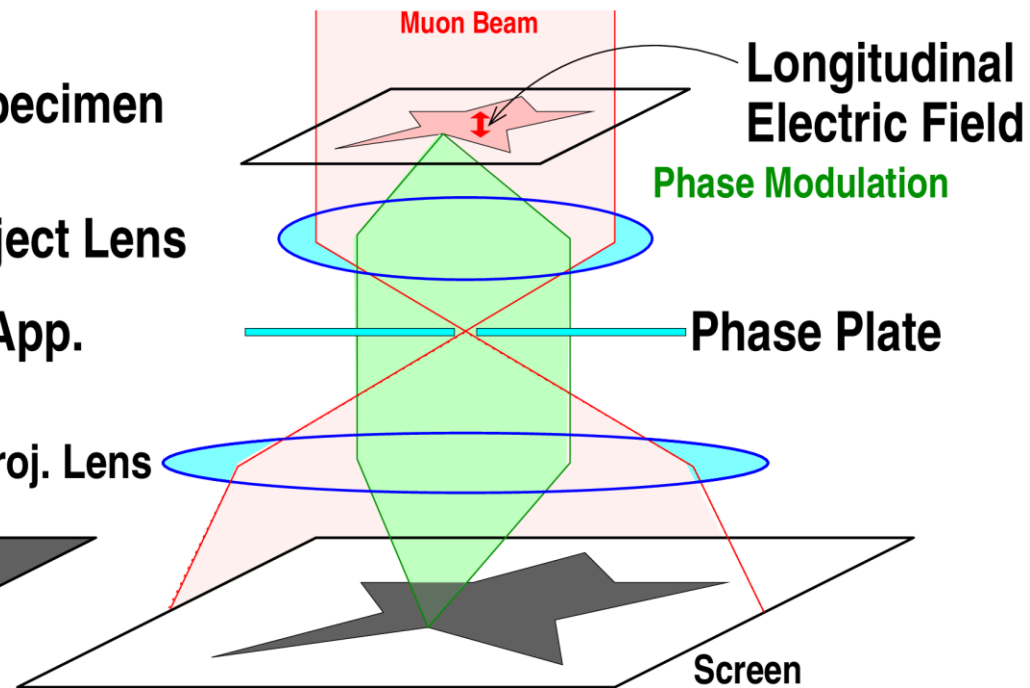
Lorentz Method

visualizes distribution of beam deflection:



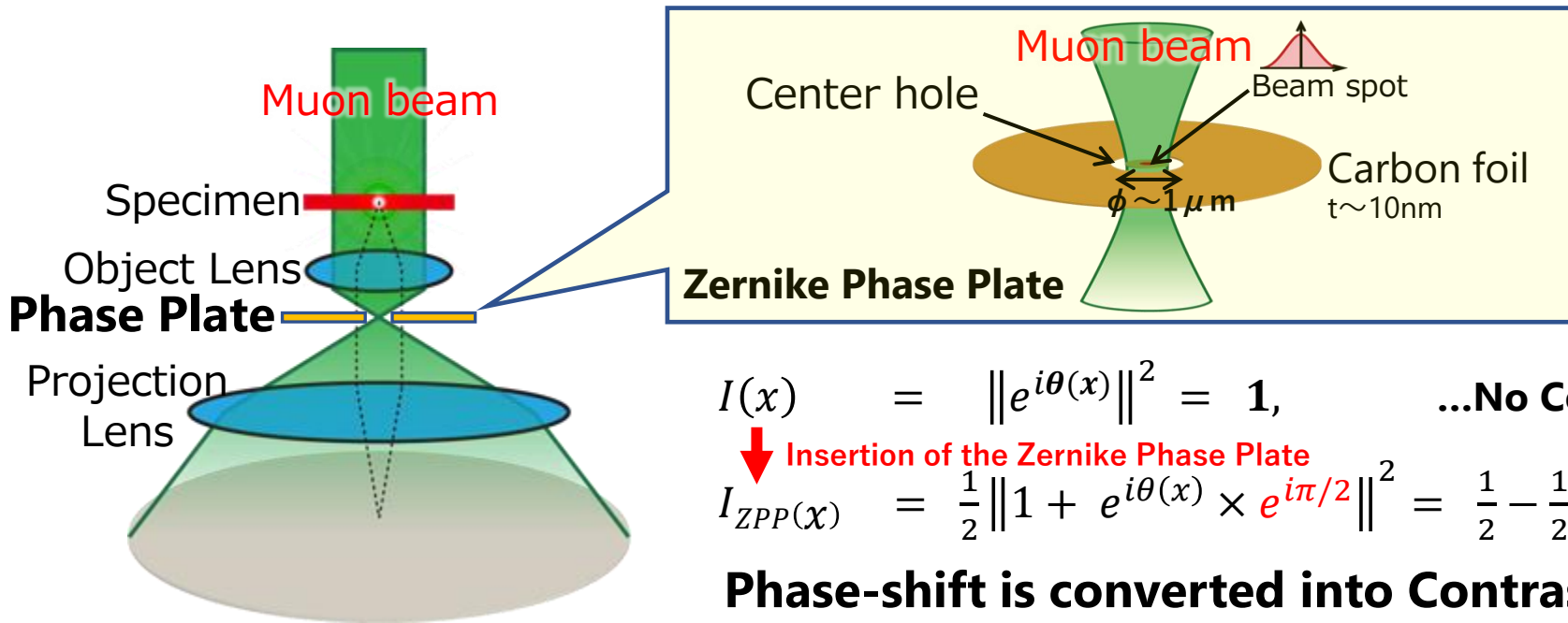
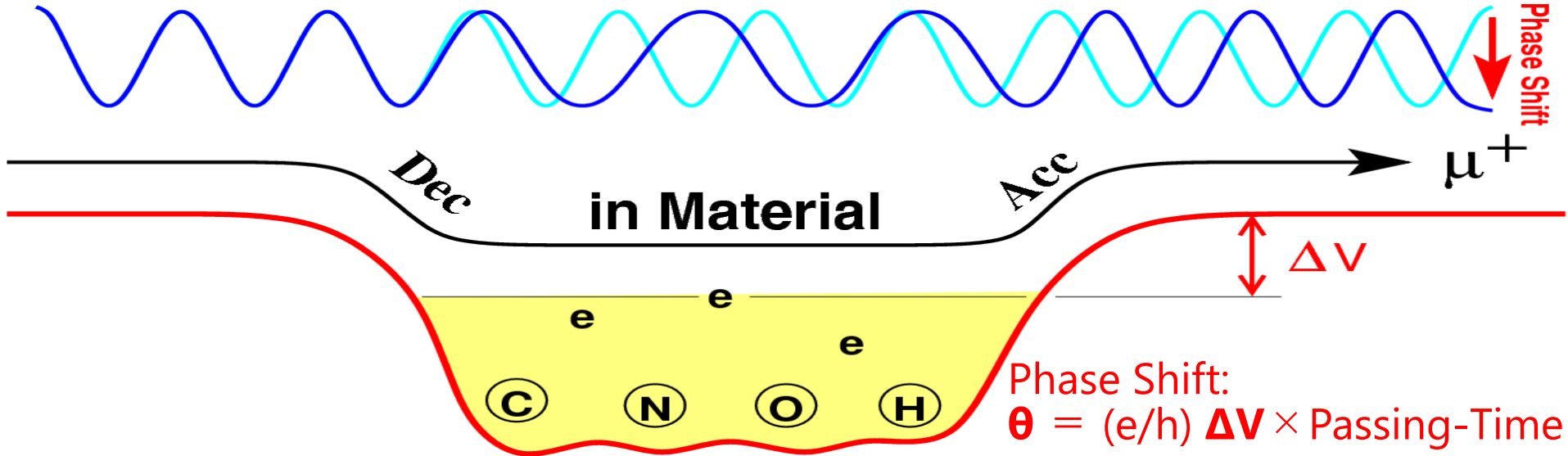
Zernike Method

visualizes electrostatic potentials:



$T\mu M$ can visualize electromagnetic field in a bulk specimen.
The 3D distribution is also obtained by Computed Tomography.

Visualization of Elec-Potential by Phase-Contrast



$$I(x) = \|e^{i\theta(x)}\|^2 = 1, \quad \dots \text{No Contrast}$$

↓ Insertion of the Zernike Phase Plate

$$I_{ZPP}(x) = \frac{1}{2} \|1 + e^{i\theta(x)} \times e^{i\pi/2}\|^2 = \frac{1}{2} - \frac{1}{2} \sin \theta(x).$$

Phase-shift is converted into Contrast 24

Test of muon imaging by CMOS Image Sensor

- CMOS Image Sensors for TEM are too expensive for test (>100k\$).
- We have tested imaging-capability of commercial digital camera (3k\$) Nikon Z7II.

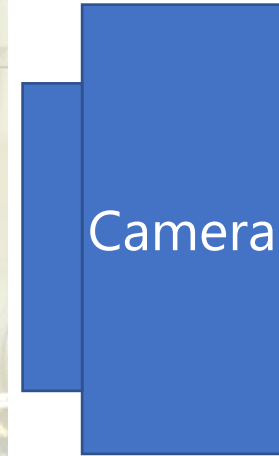
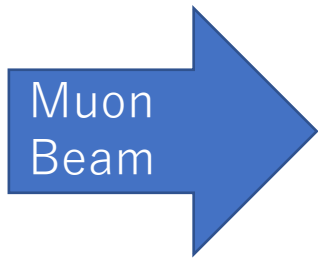


Specification :

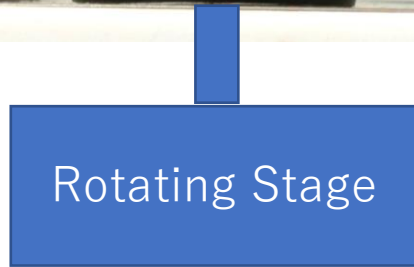
Sensor	Color CMOS Sensor, Nikon FX format
Size	35.9 × 23.9 mm
Pixels	8256 × 5504、 43 μm × 43 μm

There are several objects which disturb incoming muons on the sensor:
vibration plate for dust-cleaning, low pass filter, Infra red filter, glass window, and color filter.

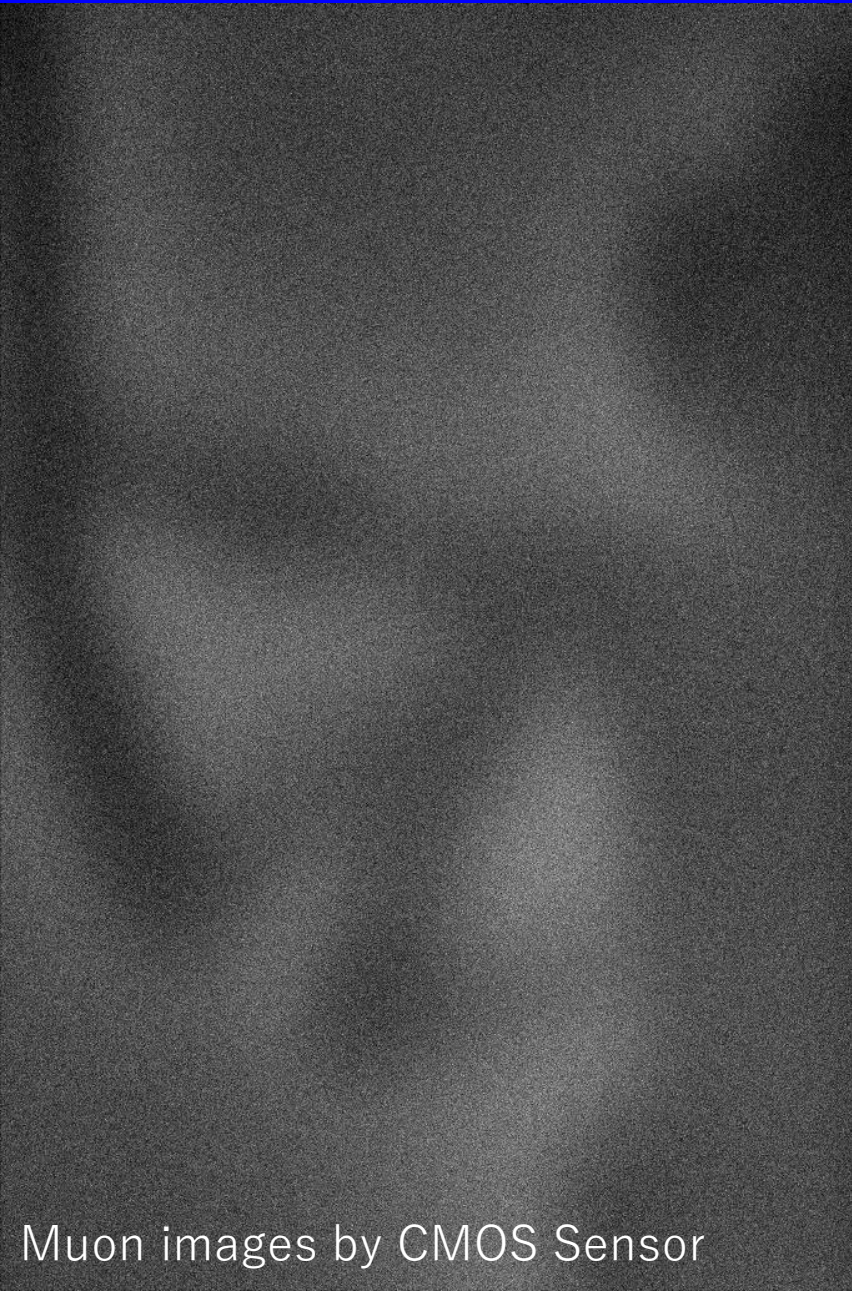
Set-up of the test



Muon beam is directly projected into the sensor without any fluorescent screen



Detected Images



000 Img Muon images by fluorescent screen

- **RESULT :**
CMOS image sensor can detect positive muons as images.
- **We can detect each projected muon, namely, muon-counting.**
 - ➔ **Super-resolution is available.**
 - ➔ **Spatial resolution can be $< 30 \mu\text{m}$.**

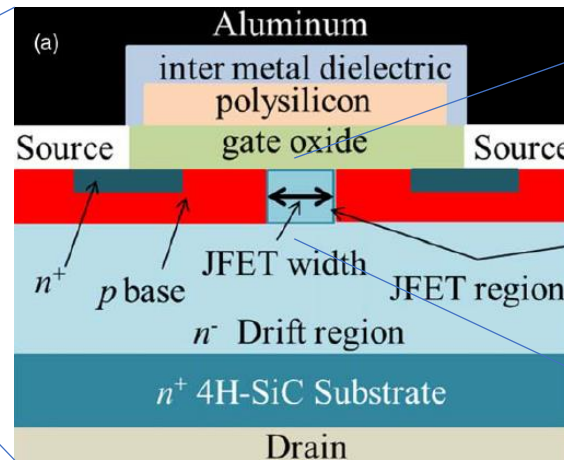
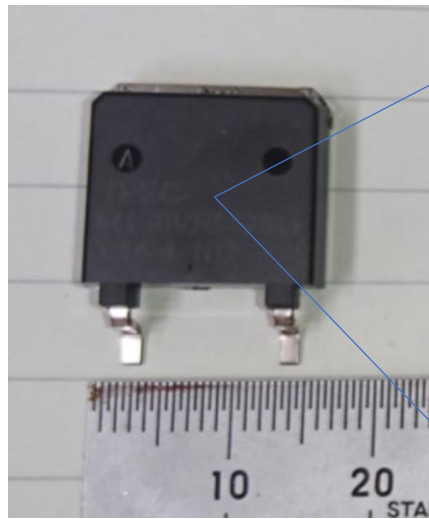


Muon images by CMOS Sensor

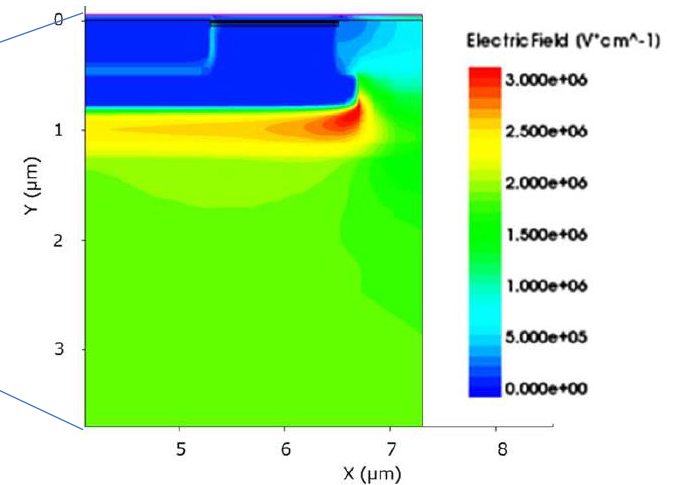
Elec-field in High Voltage Transistor (AIST)

- AIST Power Electric Group developed **14kV SiC MOS FET**.

(Highest commercial device is 3.3kV)



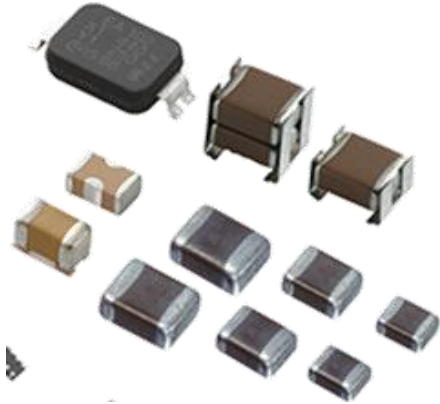
Simulated Electric Field Distrib.



- By finding points of **electric field concentration** and **break-down**, we can develop more high-voltage devices. → down-sizing, energy-saving.
- Efficient **Electric Vehicles, Power-Grids** → SDGs.
- Applicable for any power devices not only SiC but also **GaN, Ga₂O₃**.
- By GHz Stroboscopic imaging, **RF fields** are also visualized → Speed up the **communication network**, Higher performance **Rader**...

For High Performance Electric Devices

● Ceramic Condenser (MLCC)



Higher dielectric strength in unit volume is essential for market competition.

$$E = (C/2) \times V^2$$

T μ M visualizes the field concentration and break-down phenomena.

➔ It helps to develop higher performance condensers.

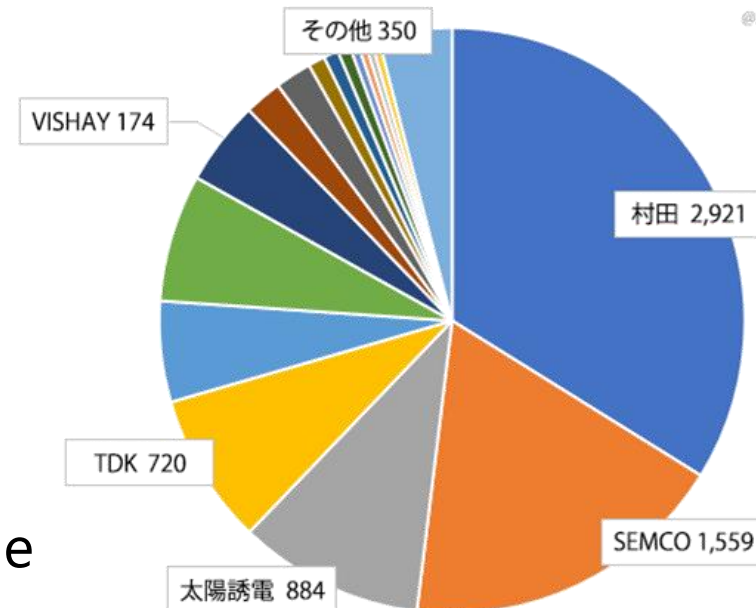
● Motor, transformer, generator

→ EV, Power Grid,

● Piezo, ultrasonic devices

→ Medical,
Non-destructive inspection.

2017 MLCC Market Shares, World : ¥8,617億



引用 : J-Chipユーザー会2018年 電子部品の供給逼迫とその対策

Applications for Material / Engineering Fields

- **Electromagnetic fields in Semiconductor Devices.**

IC, LSI, Memory, RF semiconductor devices, Reverse engineering of packaged devices.

- **Electromagnetic field in Li ion Battery.**

Visualization of inside during (dis)charging.

- **Electric fields in Piezo Devices**

Ultrasonic transmitter, US-motor, US-actuator.

- **Magnetic field in permanent magnet.**

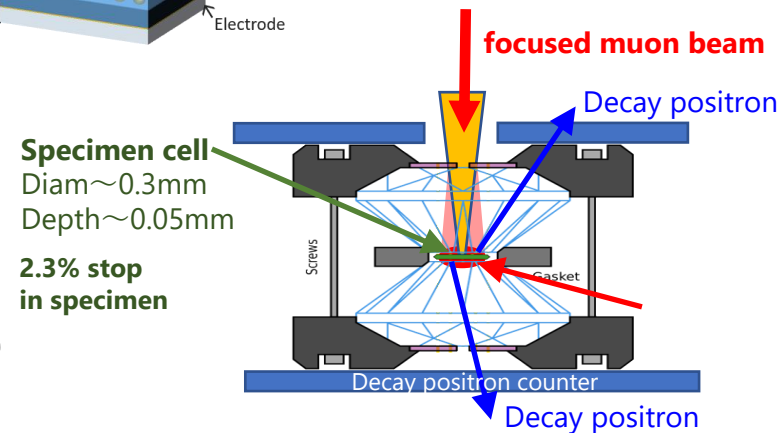
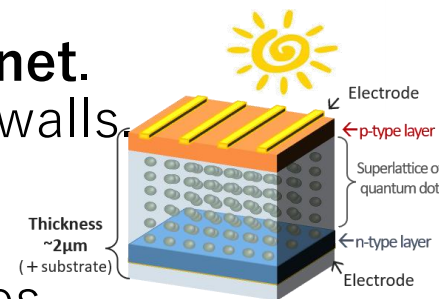
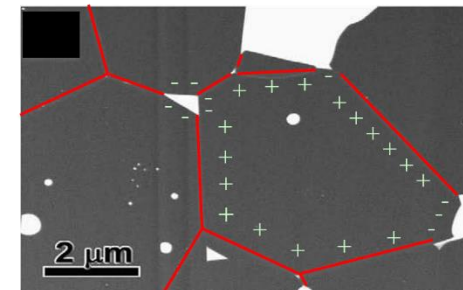
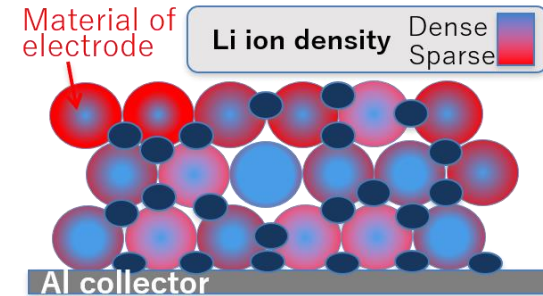
Visualization of grains and domain walls.

- **Electric field in Quantum dots.**

Solar cell, display, plasmonic devices.

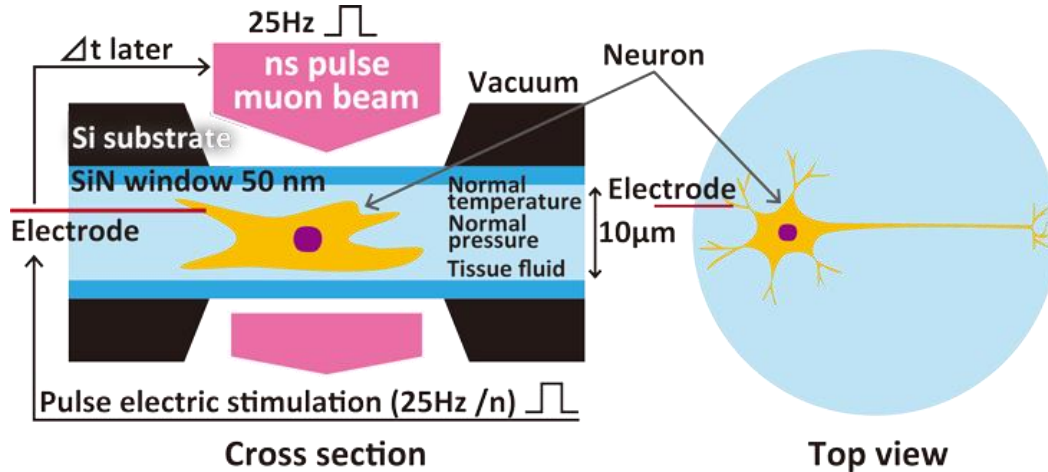
- **μ SR in a diamond anvil cell**

for room temperature Superconductors like CH_8S . (Planned at Phase-2 at H-line)



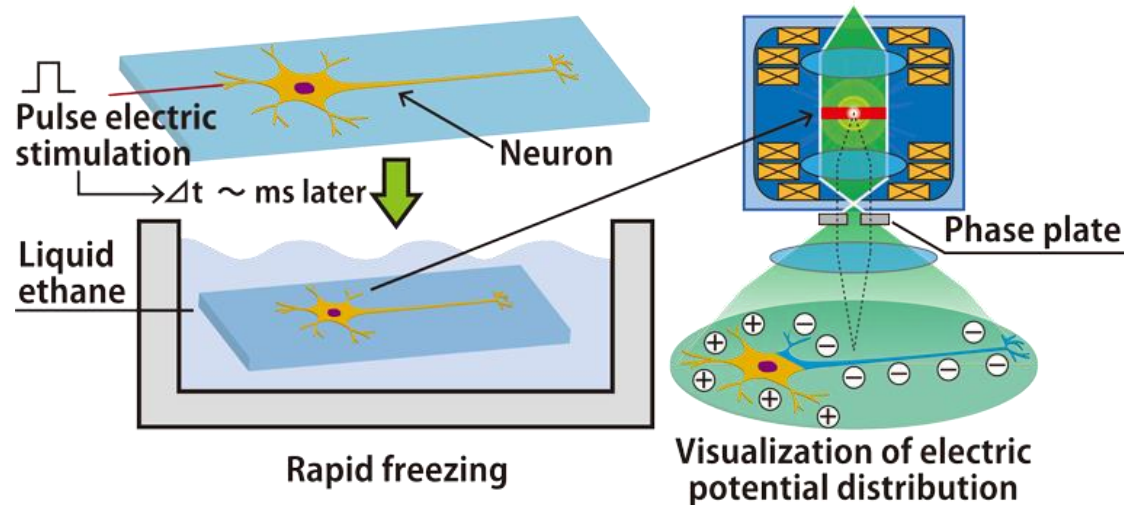
Functional Visualization of Neurons by T μ M

Stroboscopic Visualization of Action-Potential Propagation in Living Neurons in Environmental Cell



- Visualization of living neurons/networks.
- Live cells/organs in an environmental cell. in bio-liquid at room temp and pressure with windows.
- Electric pulse stimulation is synchronized with the muon pulse.
- Timing delayed Δt is scanned.

3D Tomography of Action-Potential in Neurons frozen just after an electrical stimulation

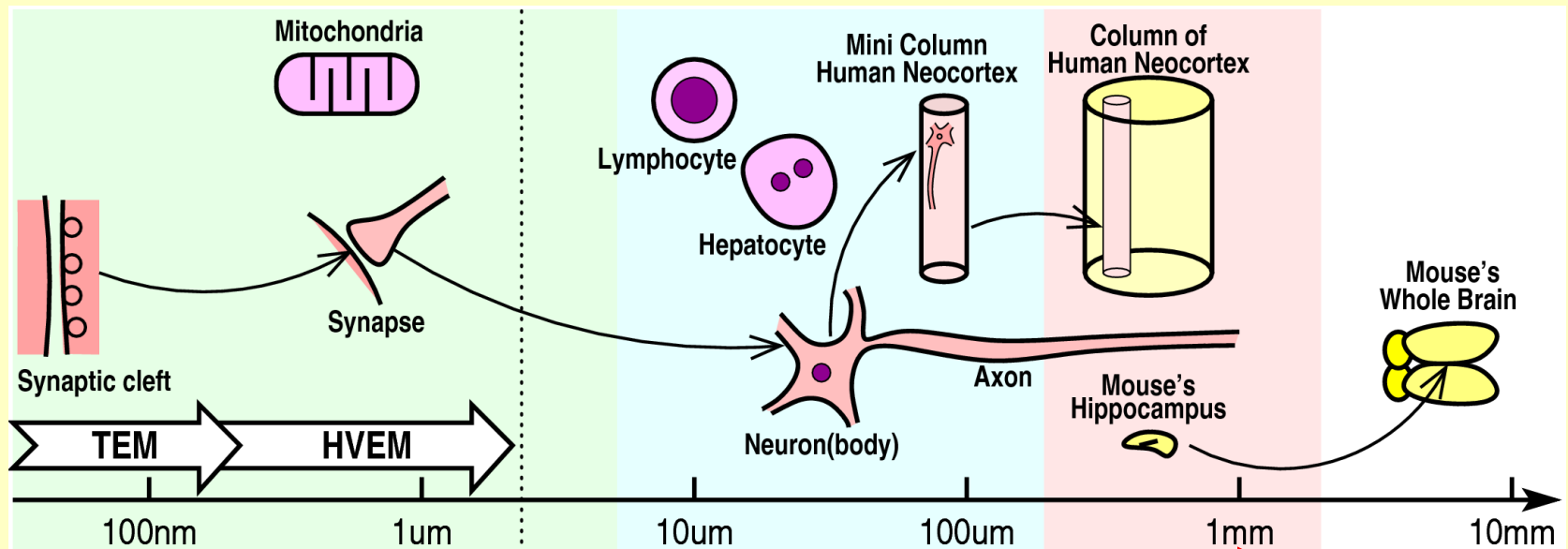


- The neuron are cultured on the electric microscope grid.
- Freezing rapidly with liquid ethane just after an electric pulse stimulation to a neuron..)
- T μ M with cryo-holder and stage.
- 3D measurement by the tomography of phase contrast.

Functional Visualization of Neurons by T μ M

Our Goal in Life Science :

Integrated / unified understanding among multi-layers:
synaptic level / neuron level / network level / organ level.

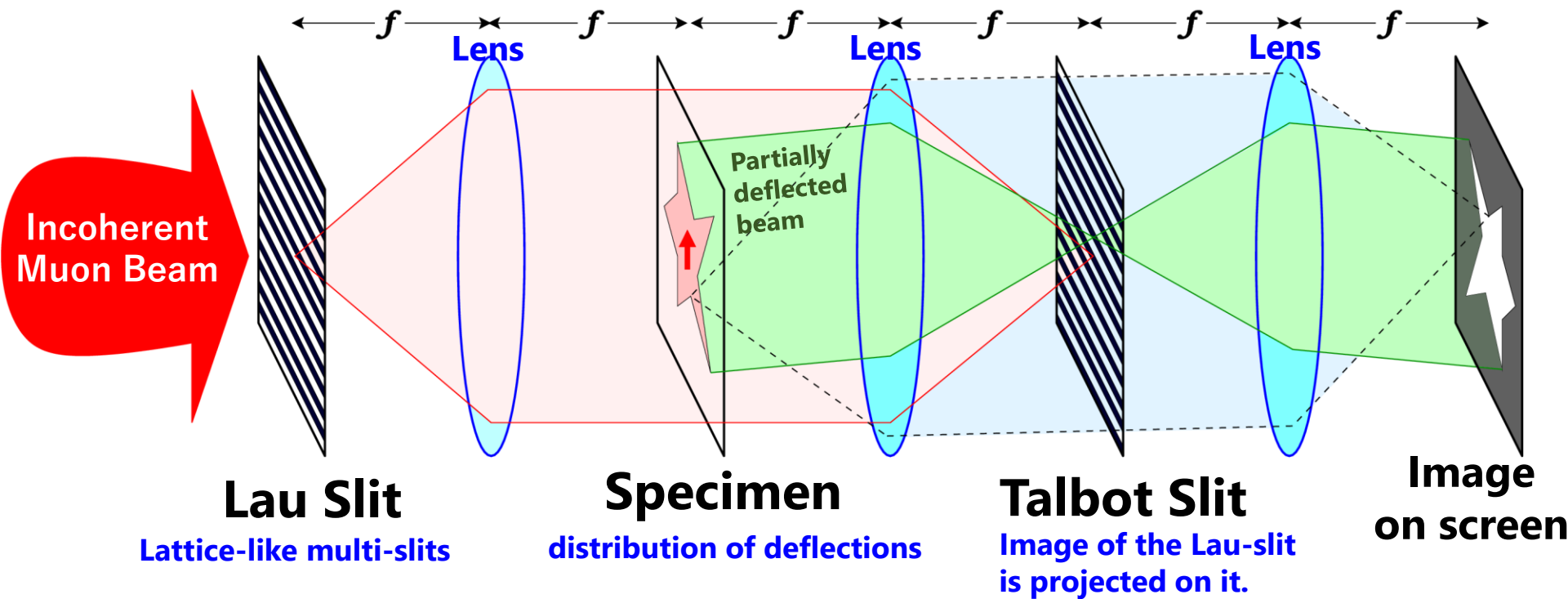


Transmission Muon Microscopy

T μ M becomes really important method for brain / bio sciences.

Phase-X: EM-Fields Imaging for Industrial Use

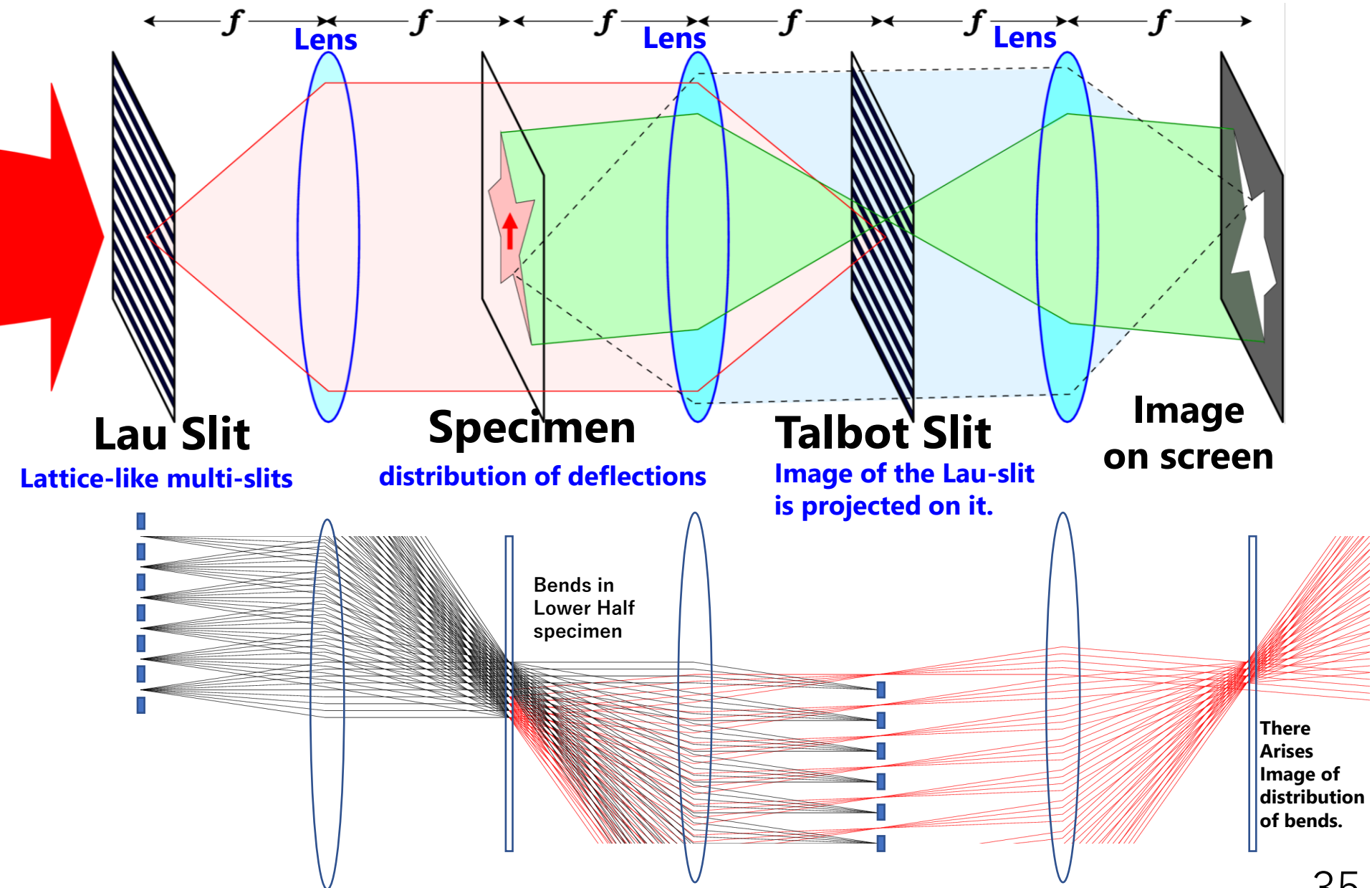
Visualizing distribution of beam-deflection by specimen.
It uses accelerator-generated muon beam directly:



- Beam cooling and re-acceleration is not required.
- While resolution is limited $\sim 3\mu\text{m}$, cm object can be observed

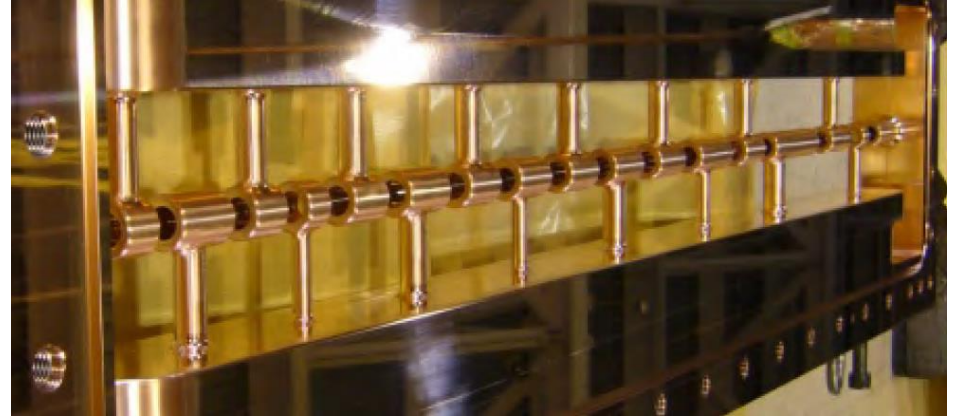
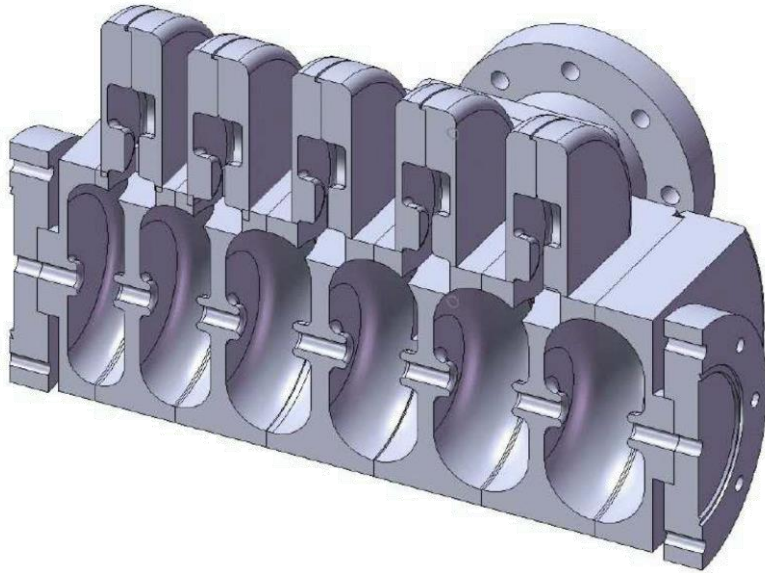
Work of the Method

Lorentz-like and Talbot-Lau-like



For High Performance Accelerator (TITech Hayashizaki)

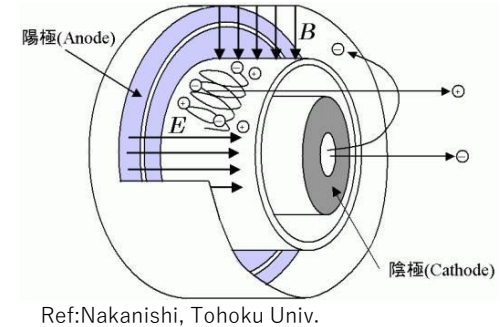
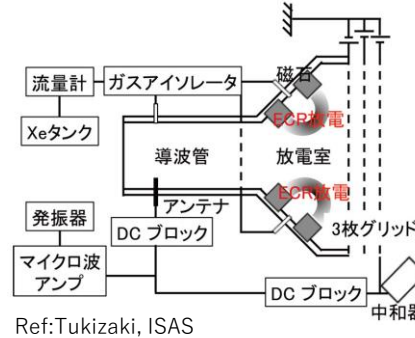
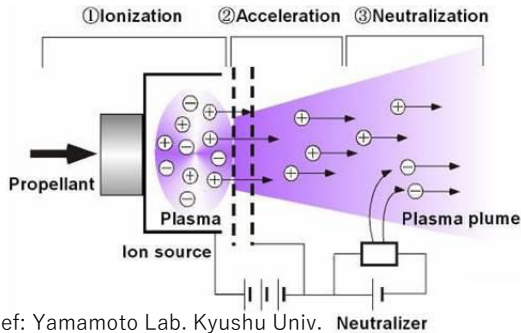
- **Particle Accelerator** uses **strong RF field** in resonant cavity.



- Higher RF field makes smaller and higher accelerator ($\sim 100\text{MV/m}$) , **Electric break-down** of high RF field limits the highest acceleration.
- Physics of the electric break-down in high RF field is unknown.
- Muon can visualize **the EM field in working accelerators**.
- **RF break-down** and **transitional phenomena** are visualized
→ Developing the ultra high performance accelerator.

For High Performance Propulsion System in Aerospace

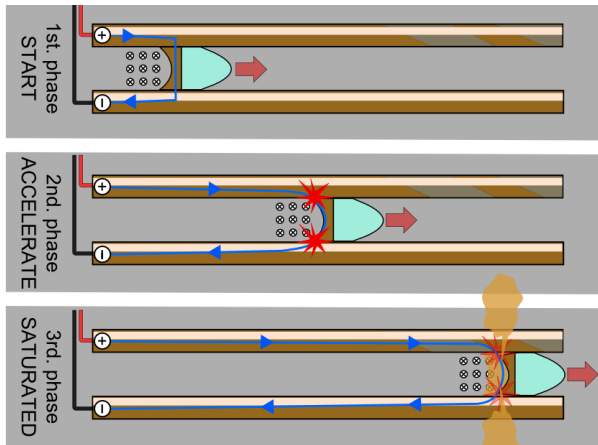
- **Ion engine / Hall thruster** : generate plasma-jet by electricity.



Complex interactions among EM/RF field and ions/electrons.
Space-charge effect limits the thrust.

➔ Measurement of **4D EM field** makes **more efficient** and **more thrust**.

- **Rail-gun** : An acceleration system by Lorentz force.



At high velocity ($\sim 7\text{km/sec}$), **velocity skin effect** limits the highest velocity.

Current concentration \rightarrow plasma generation \rightarrow dissipation \rightarrow velocity limit.

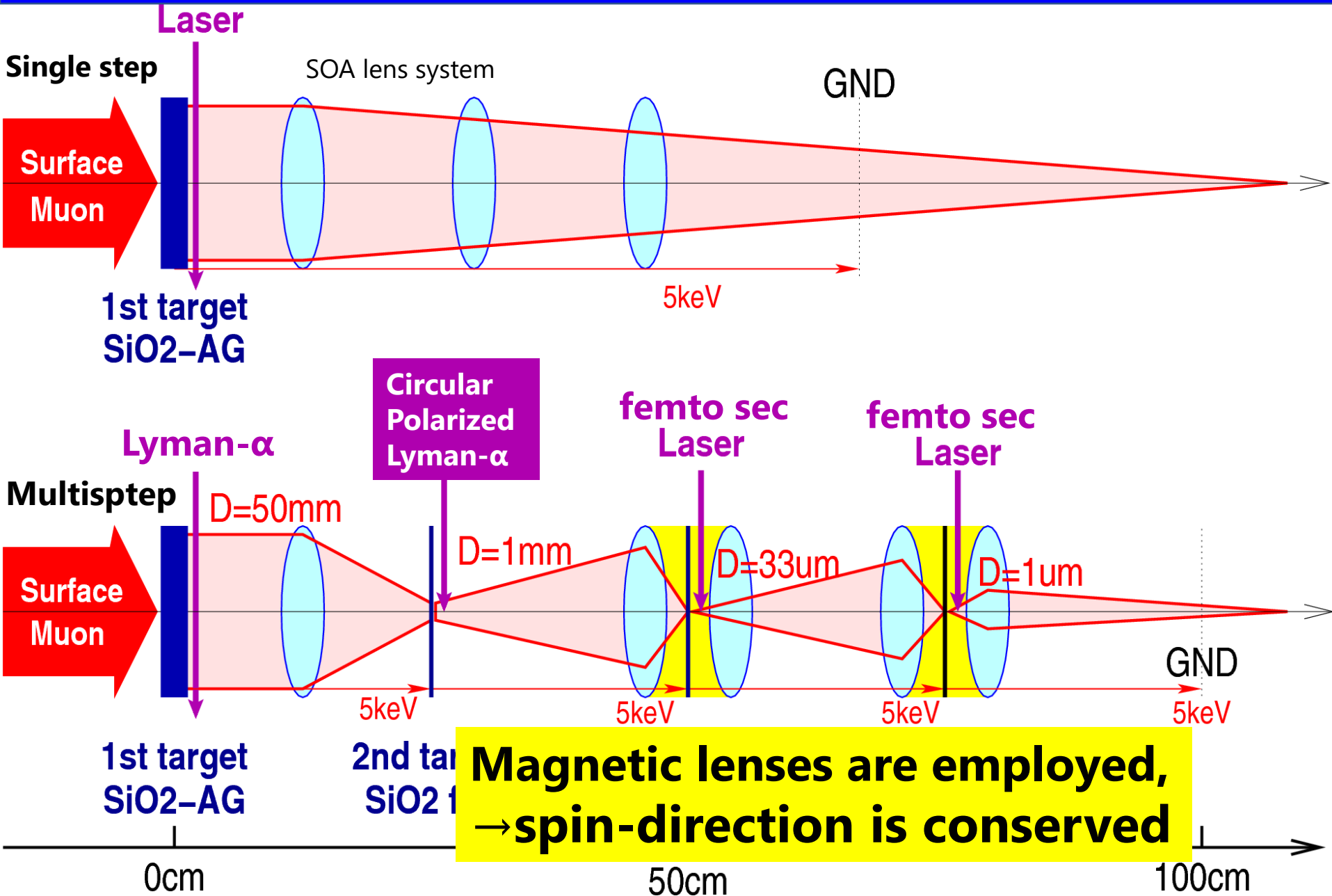
Muon visualizes the Lorentz force directly!

4D visualization of velocity skin effect makes design of **higher velocity Rail-gun**.

S μ^+ M: **Scanning positive-muon Microscopy**

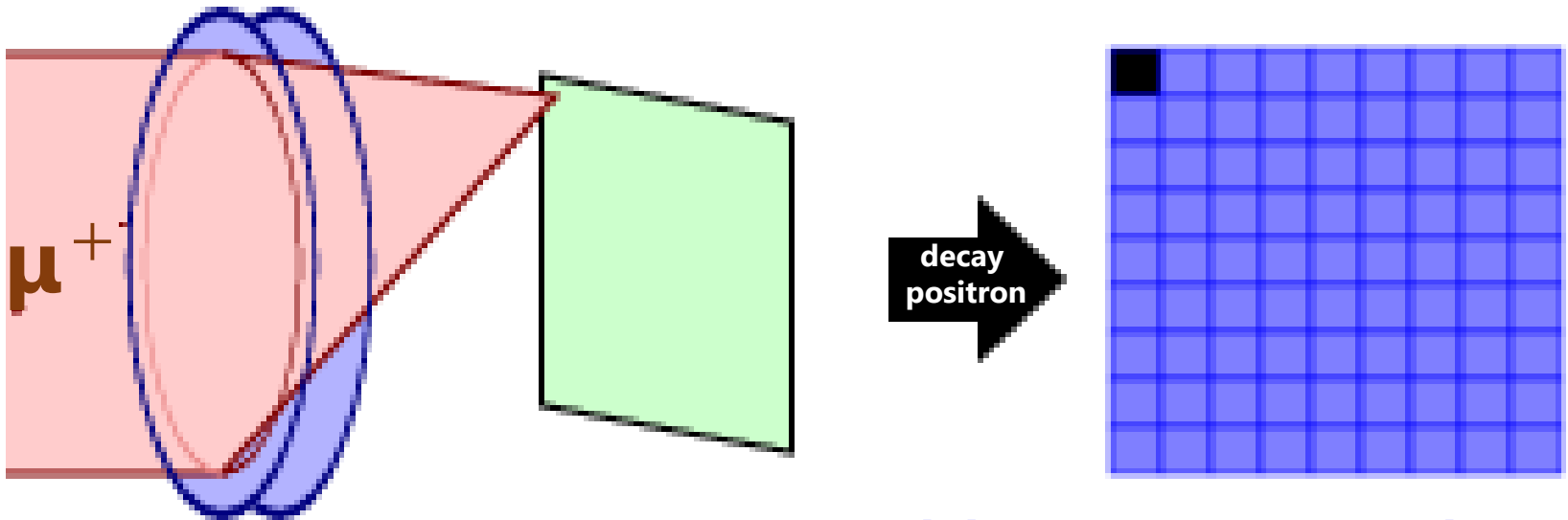
Nano-resolutional **2D/3D mapping** of
 μ SR spectroscopy on/in specimens

Muon spin polarization maintained Cooling



Scanning positive Muon Microscopy: S μ^+ M

Specimen is Scanned by focused μ^+ beams,



*and decay positrons are detected
for μ SR Spectroscopy*

**It works as a Scanning μ SR Microscope:
 μ SR Spectrum is obtained point by point!**

**3-dim mapping of magnetic field and its fluctuation,
density of Fermi surface, state of hydrogen, and etc.,
in Nano/Micro Resolutions.**

Members



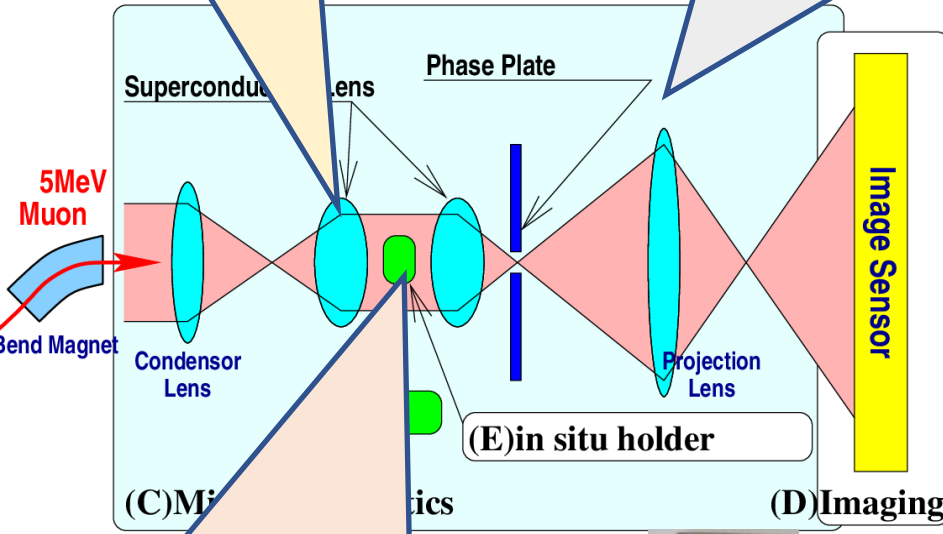
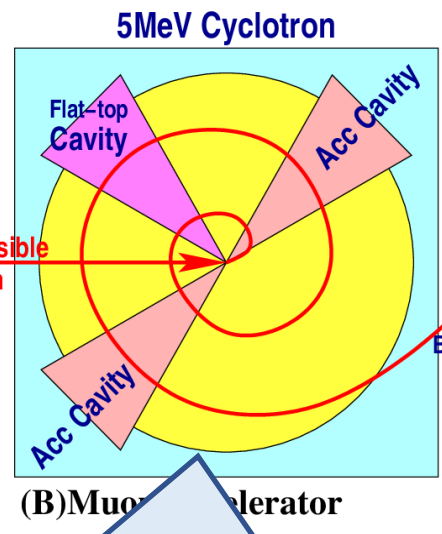
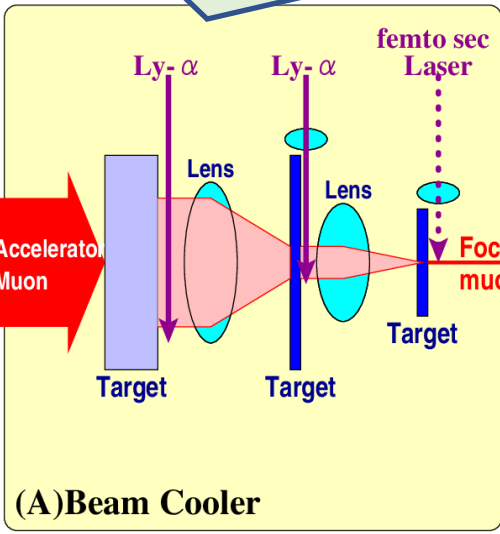
Direction : Y.N (KEK、 Fusion of Microscopies and Accelerators)

Laser Devices :
Yu Ohishi (KEK、 Lyman- α Devices) 、
Shinki Nakamura (Ibaraki U.、 Yb:YAG Laser)

Superconducting Lens :
Kenich Sasaki
 (KEK Cryo-G、 SC-Magnets)



Optics :
 Y.N.



Cyclotron and Beamlines :
Junichi Ohnishi (Riken、 Cyclotron) 、
Takayuki Yamazaki (KEK、 Beamline Develop.) 、
Akira Goto (Riken/KEK、 Cyclotron)

Power Devices :
Hiroshi Sato (AIST、 MOSFET)



Life Sciences :
N. Usuda, M. Fukazawa (Fujita Med. U, Brain),
K. Jokura, K. Kame (Shinshu U. Med.),
K. Muratra (NIPS, TEM), **T. Senda** (KEK, TEM/X-ray)

Beamline Management : Koichiro Shimomura (KEK)

Collaboration and Partners

- **KEK** Muon group: Y. N., T. Yamazaki, P. Strasser, S. Kanda, S. Nishimura, S. Matoba, Y. Ikedo, T. Yuasa, N. Kawamura, Y. Ohishi, A. D. Pant, M. Tampo, S. Doiuchi, A. Goto, K. Shimomura, Y. Miyake.
g-2/EDM group: T. Mibe et.al. (g-2/EDM collaboration)
Accelerator facility: Toshikazu Adachi, H. Someya, M. Yoshida.
Cryogenic group: T. Ogitsu, K. Sasaki, N. Kurosawa.
- **RIKEN** J. Ohnishi, Taihei Adachi.
- **Tokyo I.Tech** T. Sannomiya, N. Hayashizaki.
- **AIST** H. Sato, T. Kuroiwa, K. Sakamoto, F. Kato.
- **NIPS** K. Murata.
- **Industry** (Sumiotmo HI) K. Kumada, S. Kusuoka, K. Onda, Y. Tsutsui.
(JEOL) M. Iwatsuki, (Terabase) Y. Arai.

Summary

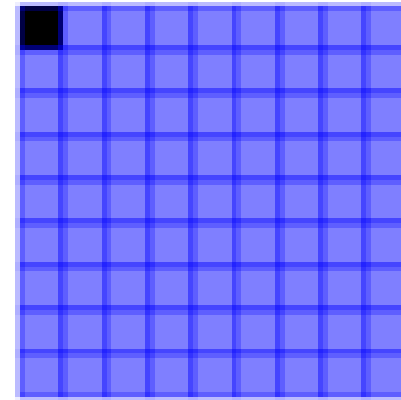
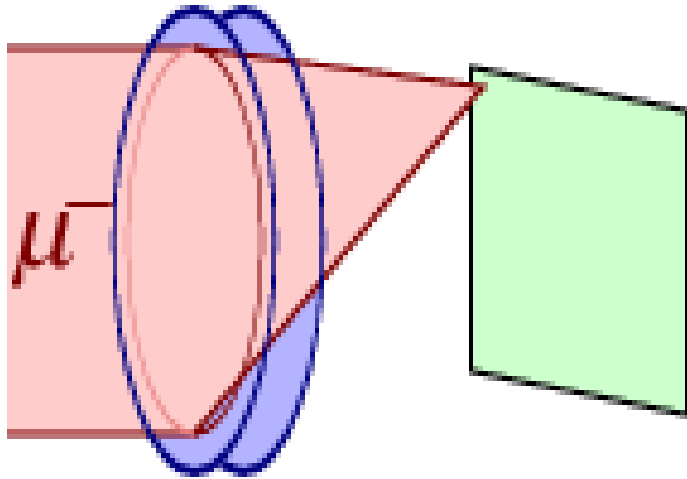
- T μ M clarifies how our brain works, by **functional imaging of macroscopic neural systems** in nanometer resolution.
- **Visualization of electromagnetic fields in bulk object** is widely applicable to material science and engineering fields, so our modern material civilization is depending on electromagnetism.

S μ^- M: **Scanning negative-muon Microscopy**

2D/3D mapping of elements
in μm -resolution

Goal of S μ -M

Specimen is scanned
by focused μ^- beam



Muonic X-ray analysis

- **2D/3D mapping of elements, isotopes and chemical situations.**
- High sensitivity for light elements
→ **Applicable to Life** consisting from C, N, O.

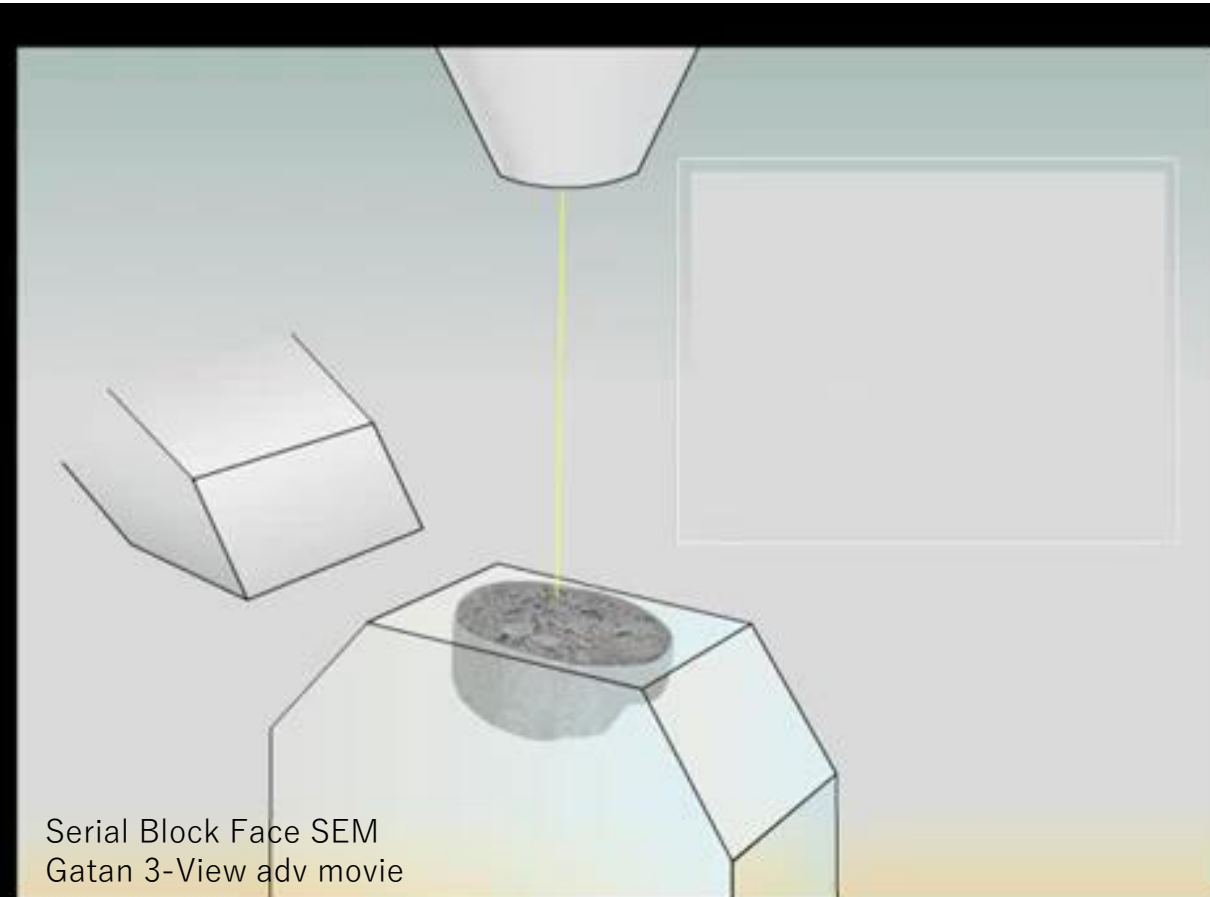
Application : 3D elemental map of Life

Comprehensive 3-dimensional mapping of elements/isotopes for life/tissues.

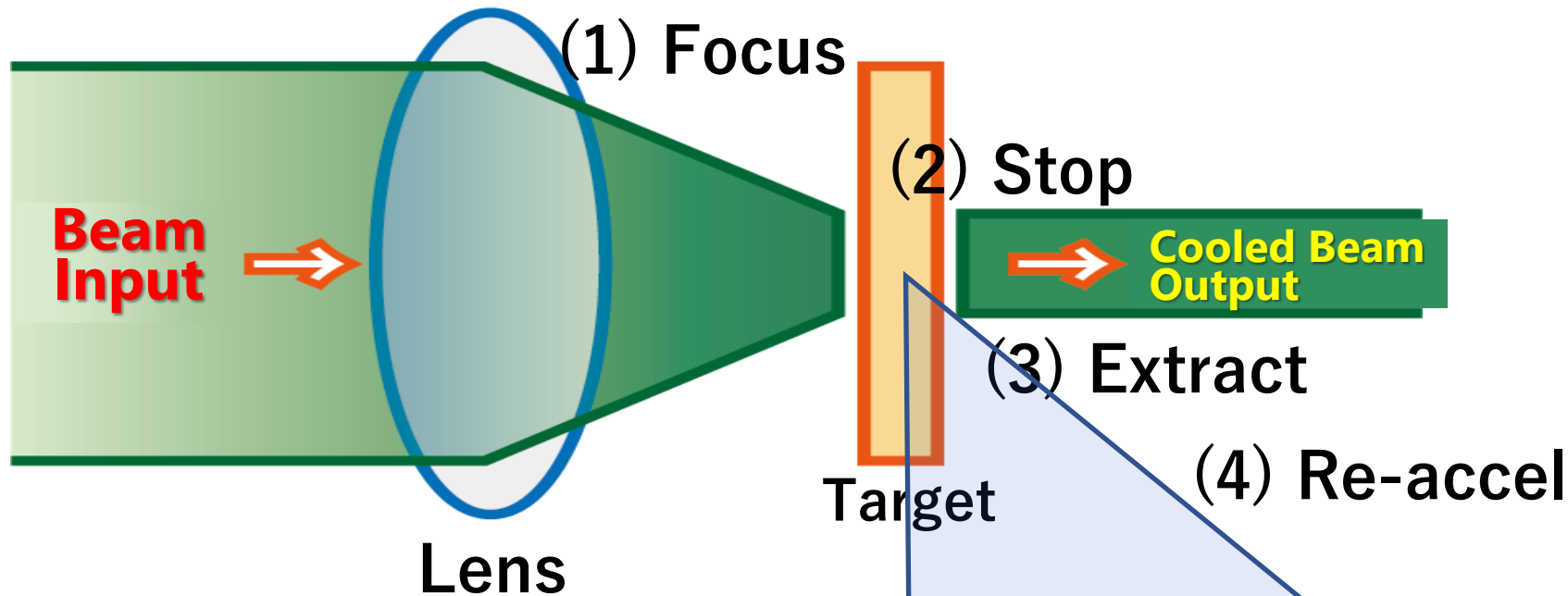
→ New generation of the life-informatics

1. Rapid freezing
2. Taking elemental images serially with cutting the frozen tissue.
3. 3-dimensional elemental map is obtained in μm resolution.

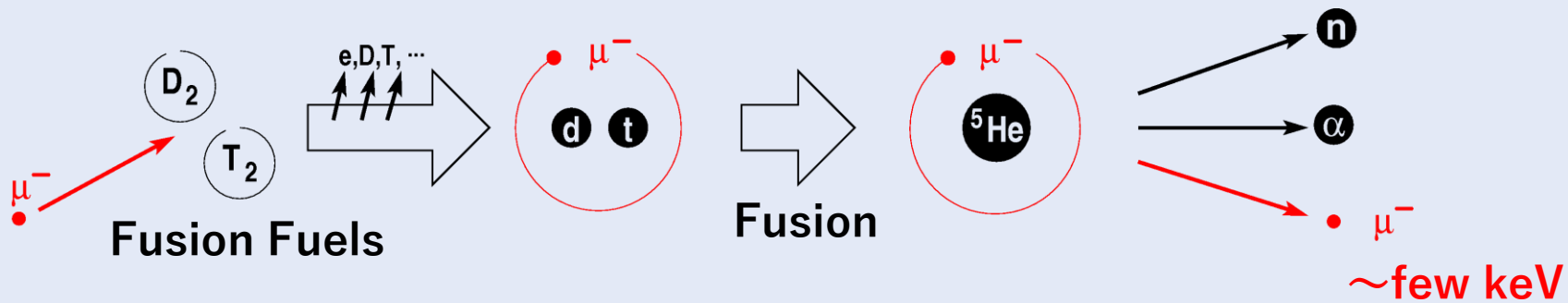
This method is a destructive measurement.



Beam Cooling of negative muon

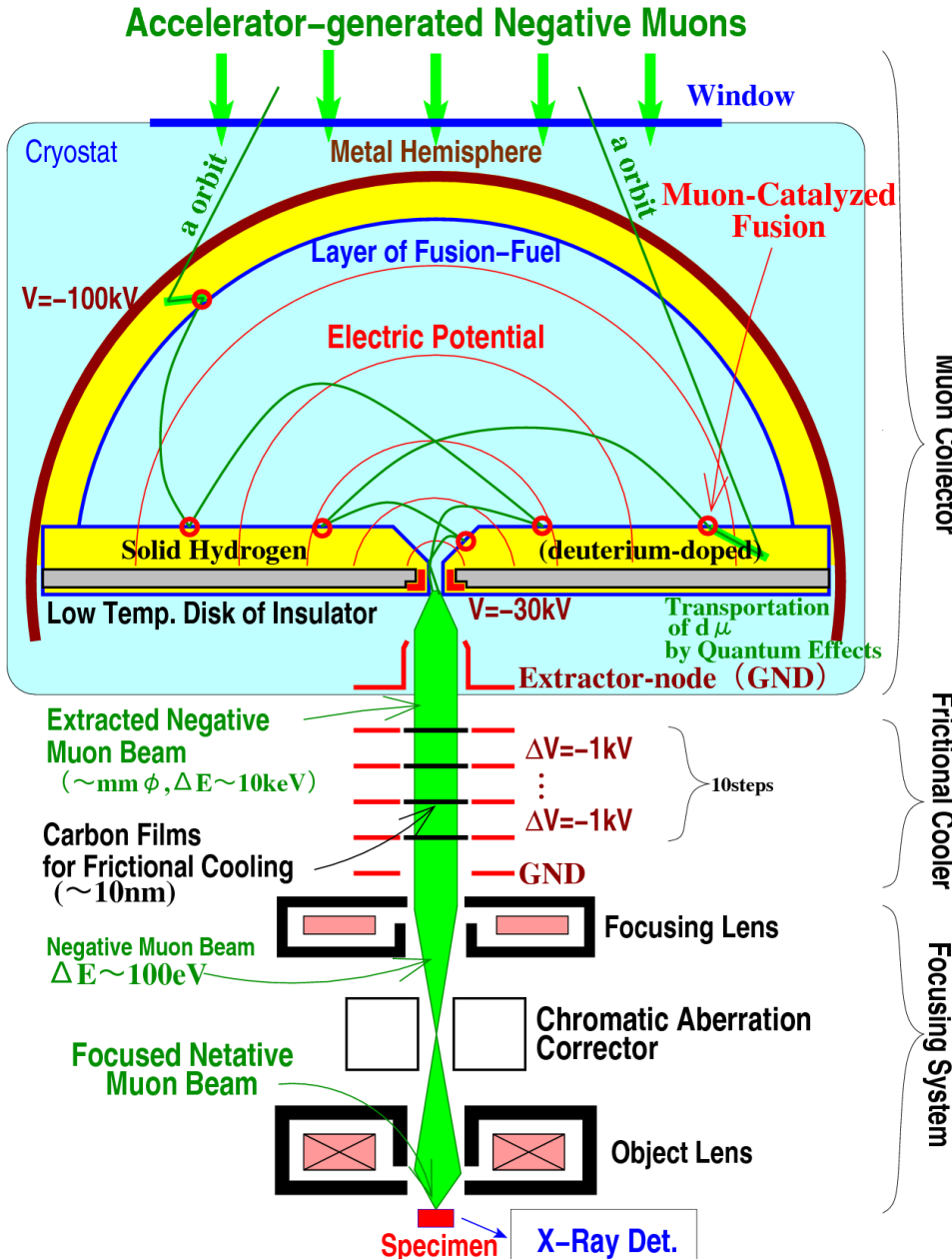


Using μCF reaction for (2) stopping and (3) extracting [Nagamine].



Low energy muons are emitted after μCF reaction.

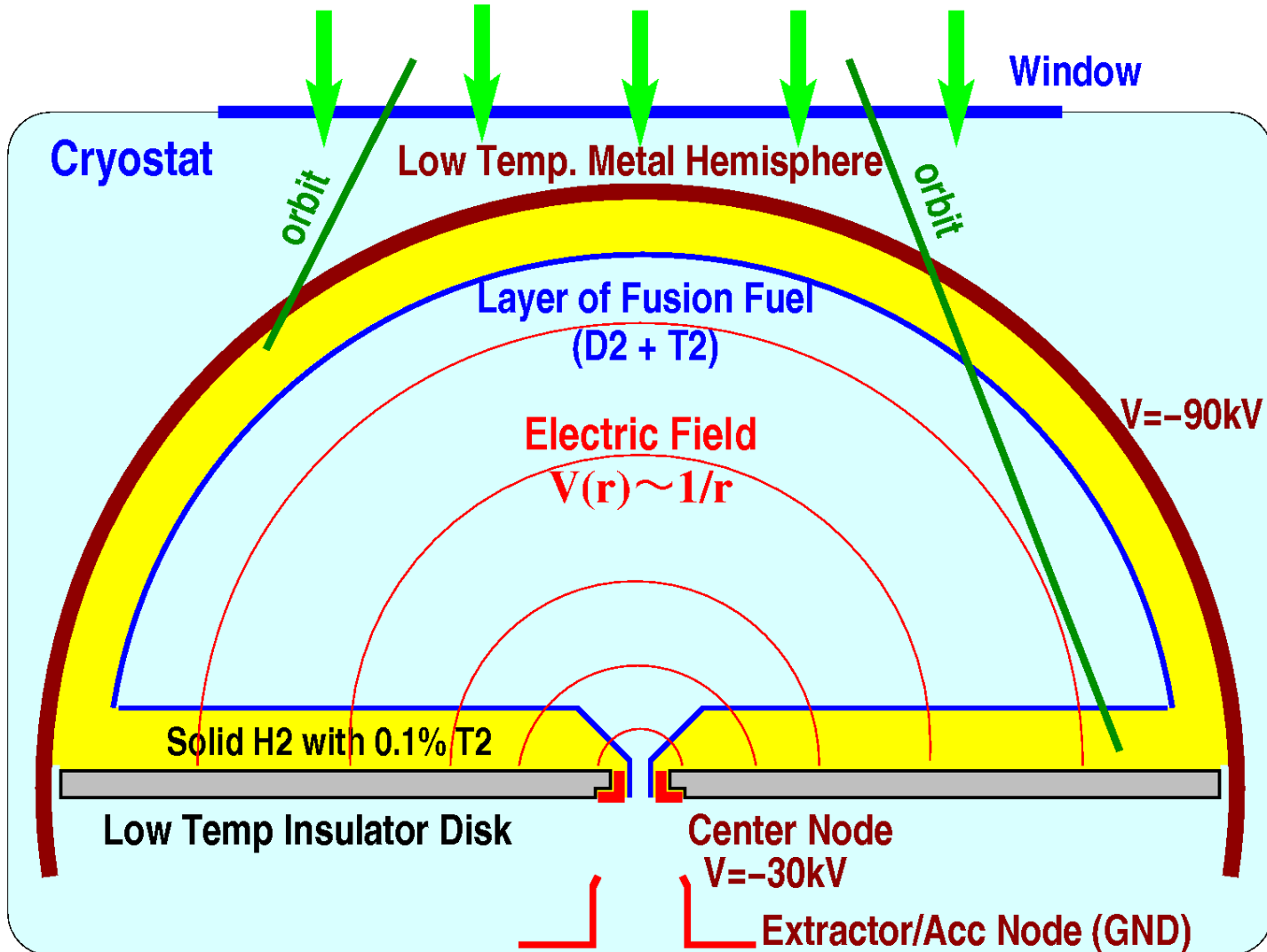
Generation of Focused neg. Muon Beam.



- 1) **Muon Catalyzed Fusion (μCF)** is applied to the beam-cooling. Captured muon into atom is dissociated with low energy $\sim 10\text{keV}$ after μCF .
- 2) Accelerator muon is captured by solid H_2 with mm-thickness. $p\mu$ is converted into $d\mu$, and $d\mu$ diffuses in mm-range by **Ramsauer-Townsend effect**.
- 3) μCF on thin DT-layer on solid H_2 dissociates the muon. The muon is transported into center by E-field.
- 4) Muon beam is extracted, is cooled frictionally, and is focused on specimen.

Negative Muon Collector

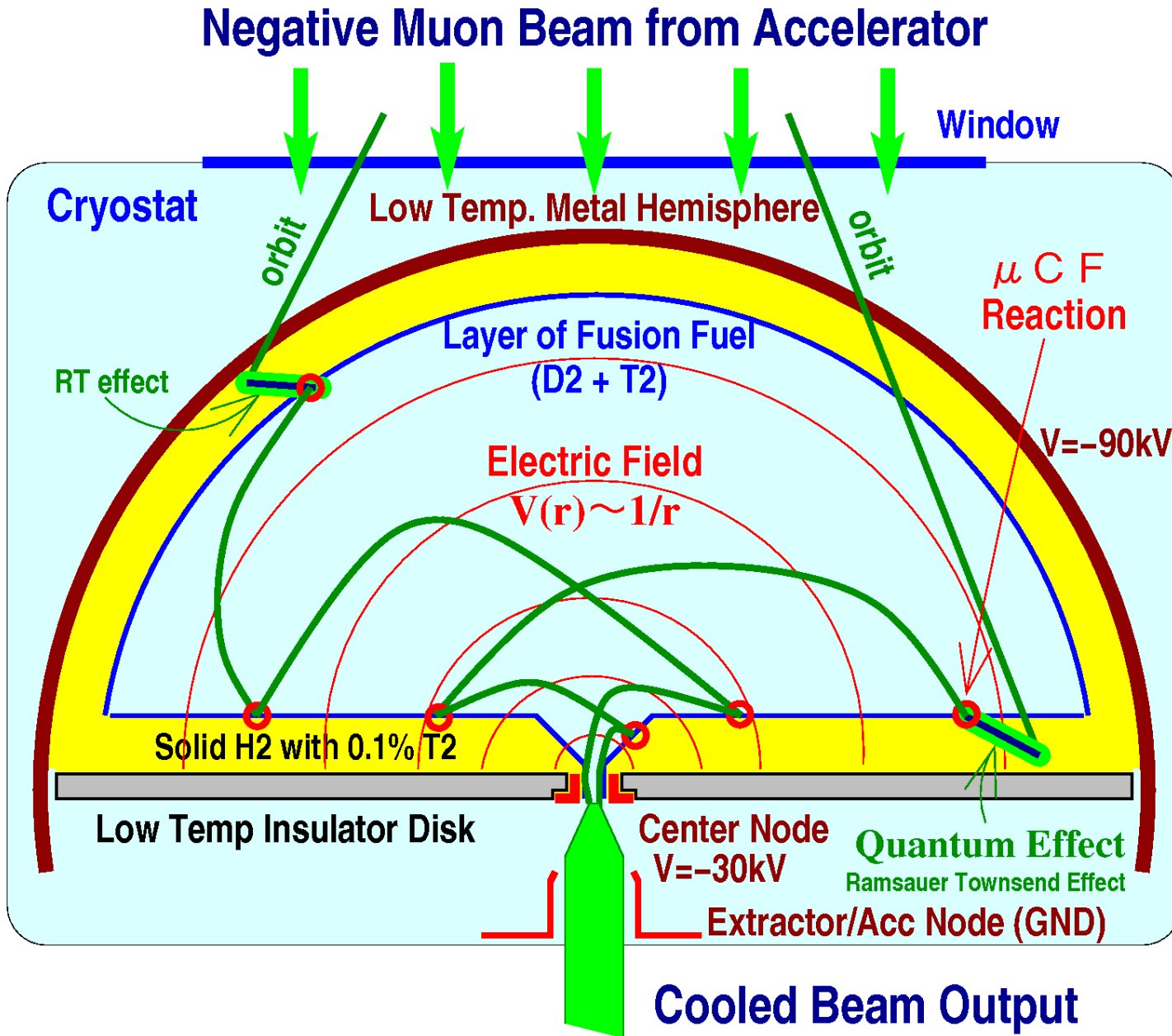
Negative Muon Beam from Accelerator



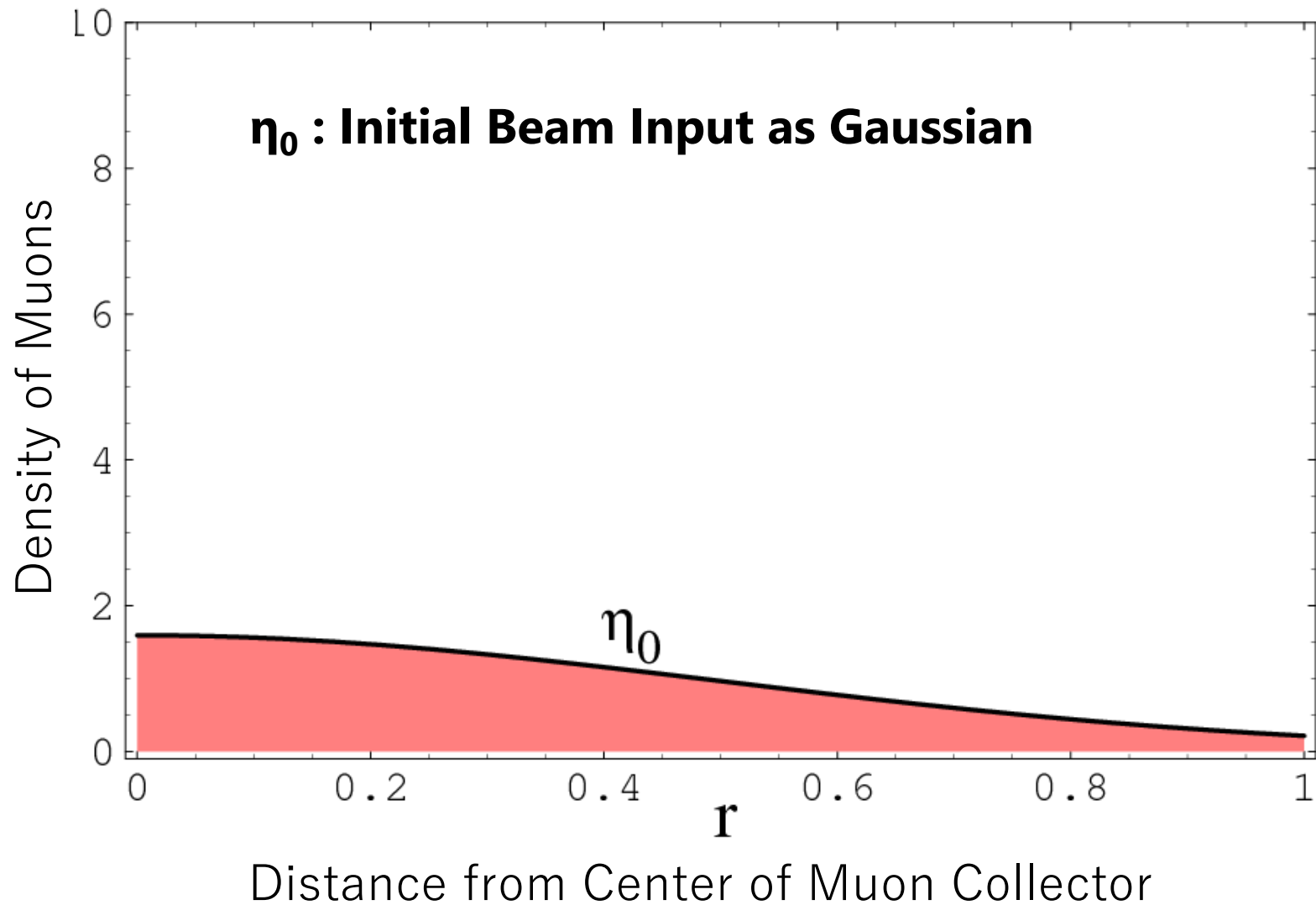
Use of Ramsauer Townsend Effect

- Solid H₂ Layer : 1mm : 99.9% **H₂** + 0.1% **T₂**,
Solid DT Layer : 1μm : 70% **D₂** + 30% **T₂**.
- Injected μ⁻ stops at Solid H₂ Layer → pμ is formed.
- Isotope exchange: pμ + t → tμ + p
tμ obtains kinetic energy around E~40eV.
- Thermally tμ relaxes into sub meV.
At the way, its scattering cross section becomes almost zero at E~1eV by Ramsauer Townsend effect.
- Finally, **tμ diffuses in sub mm range.**

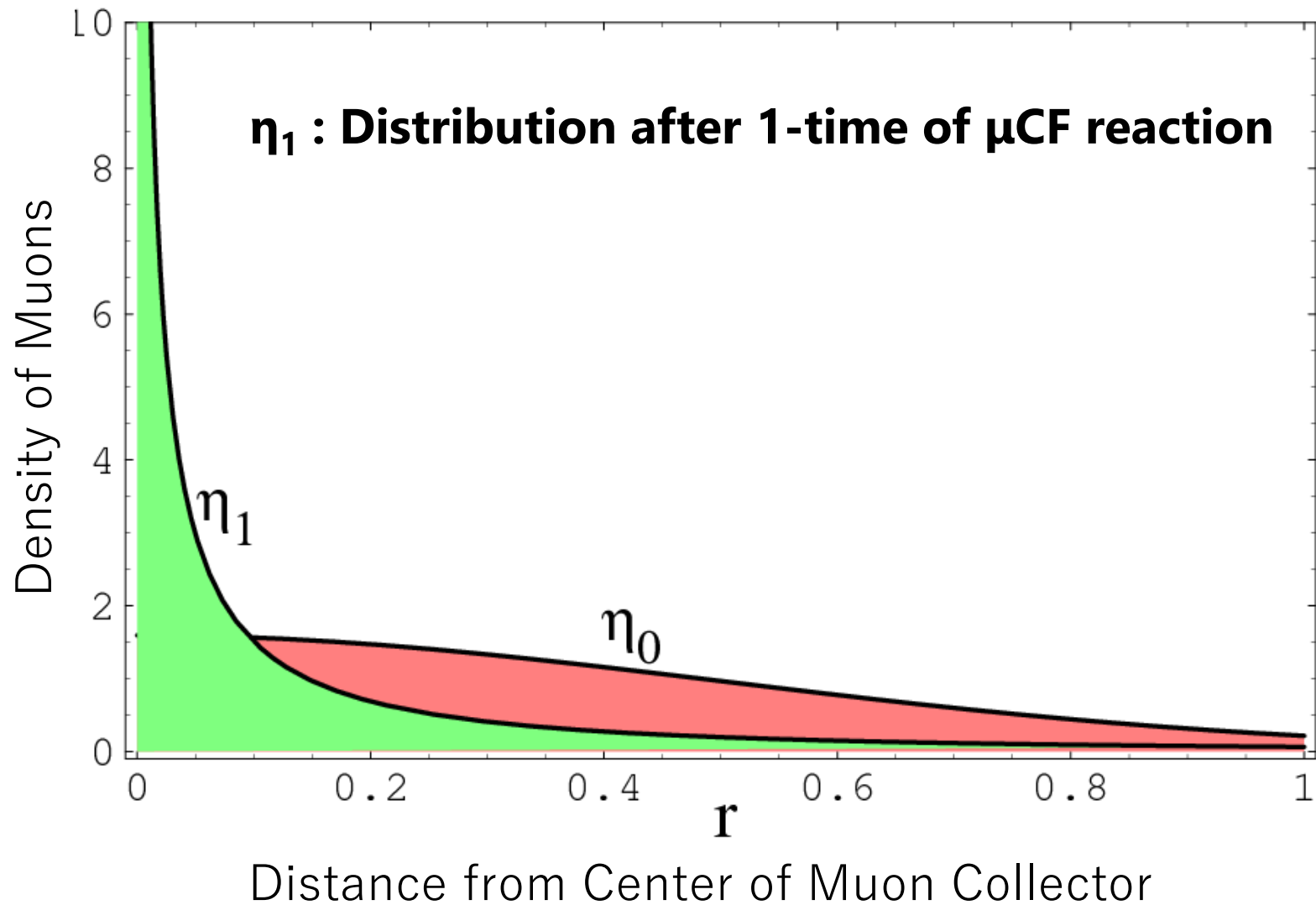
Negative Muon Collector



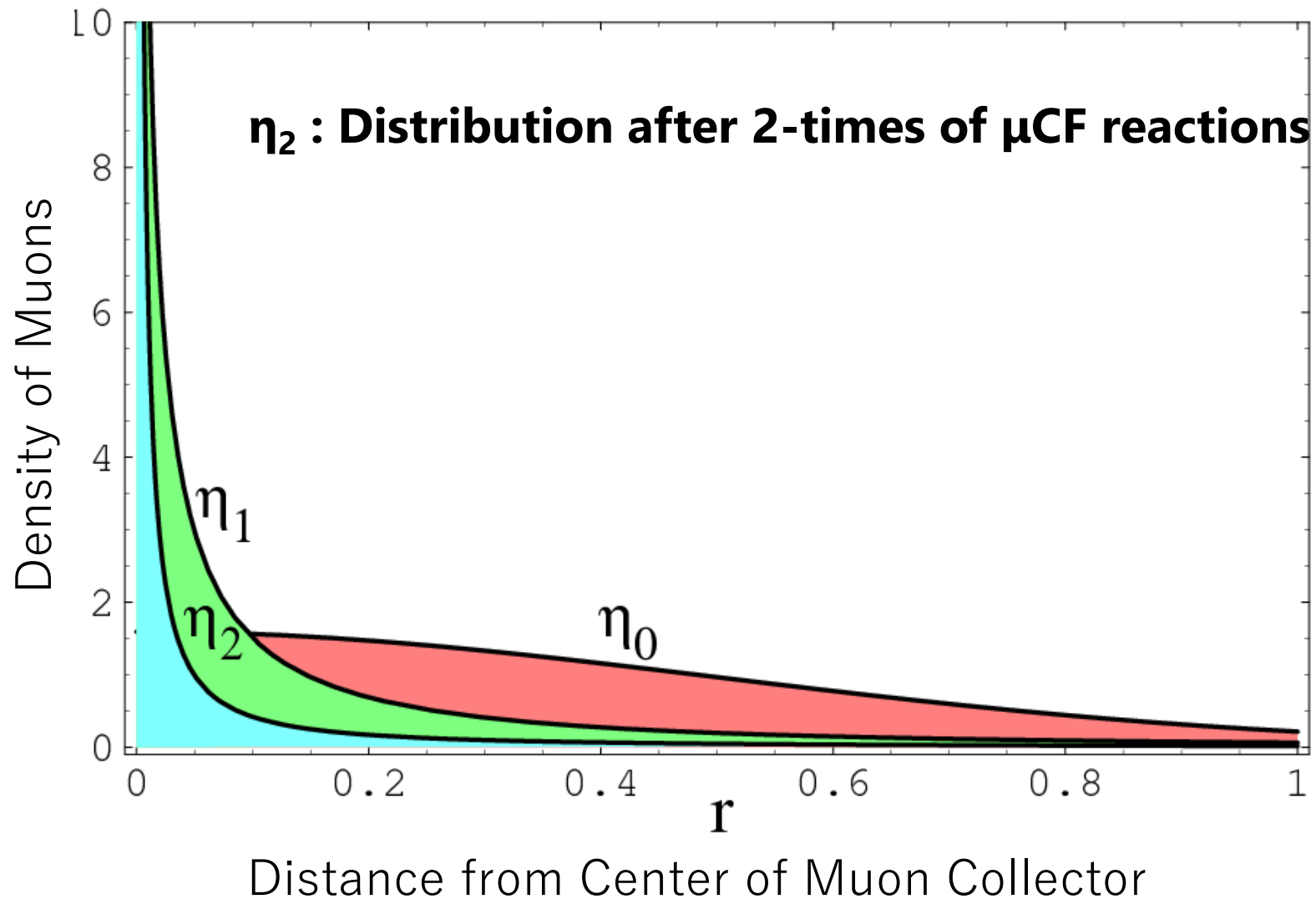
Simulation of Muon Collector



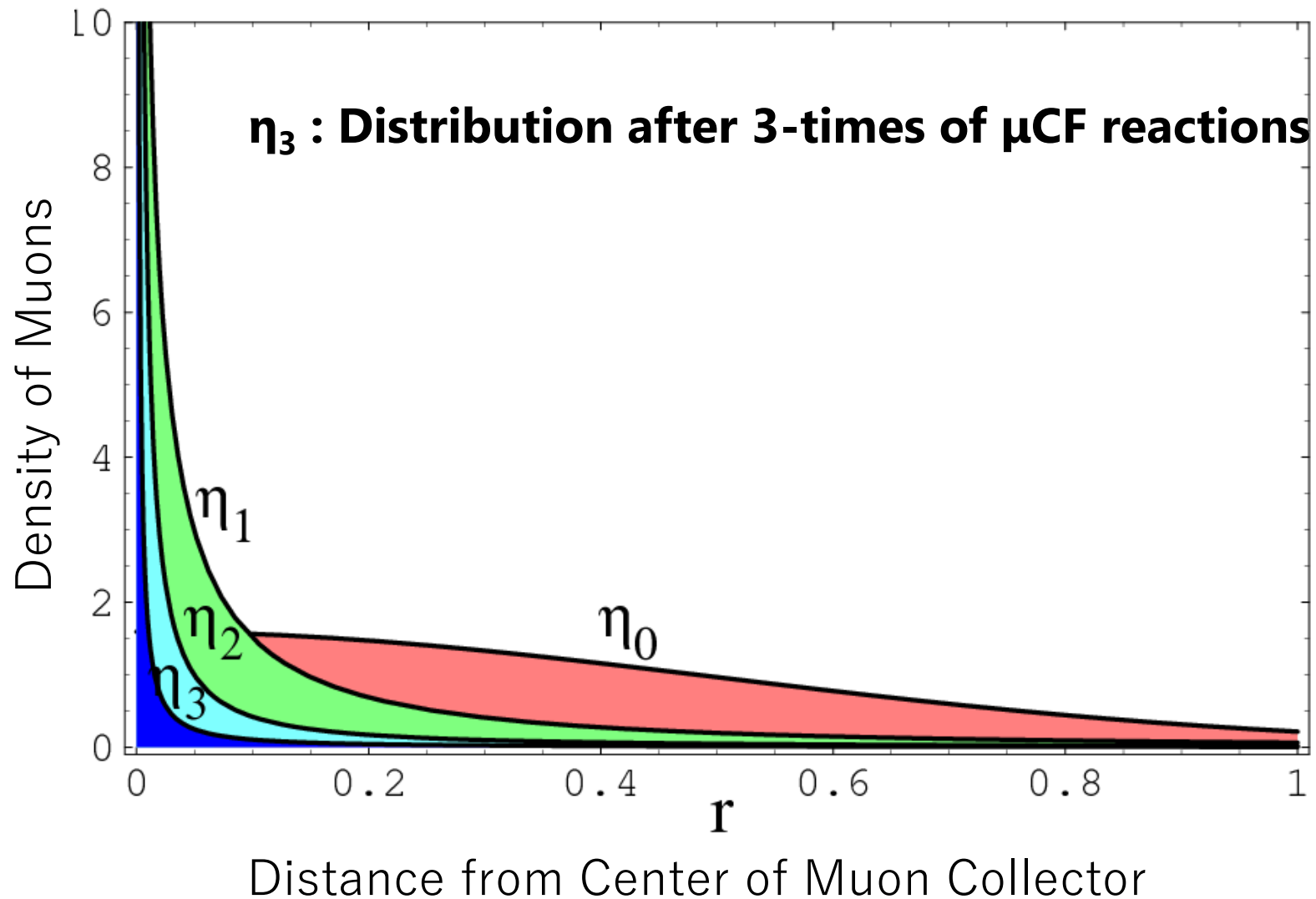
Simulation of Muon Collector



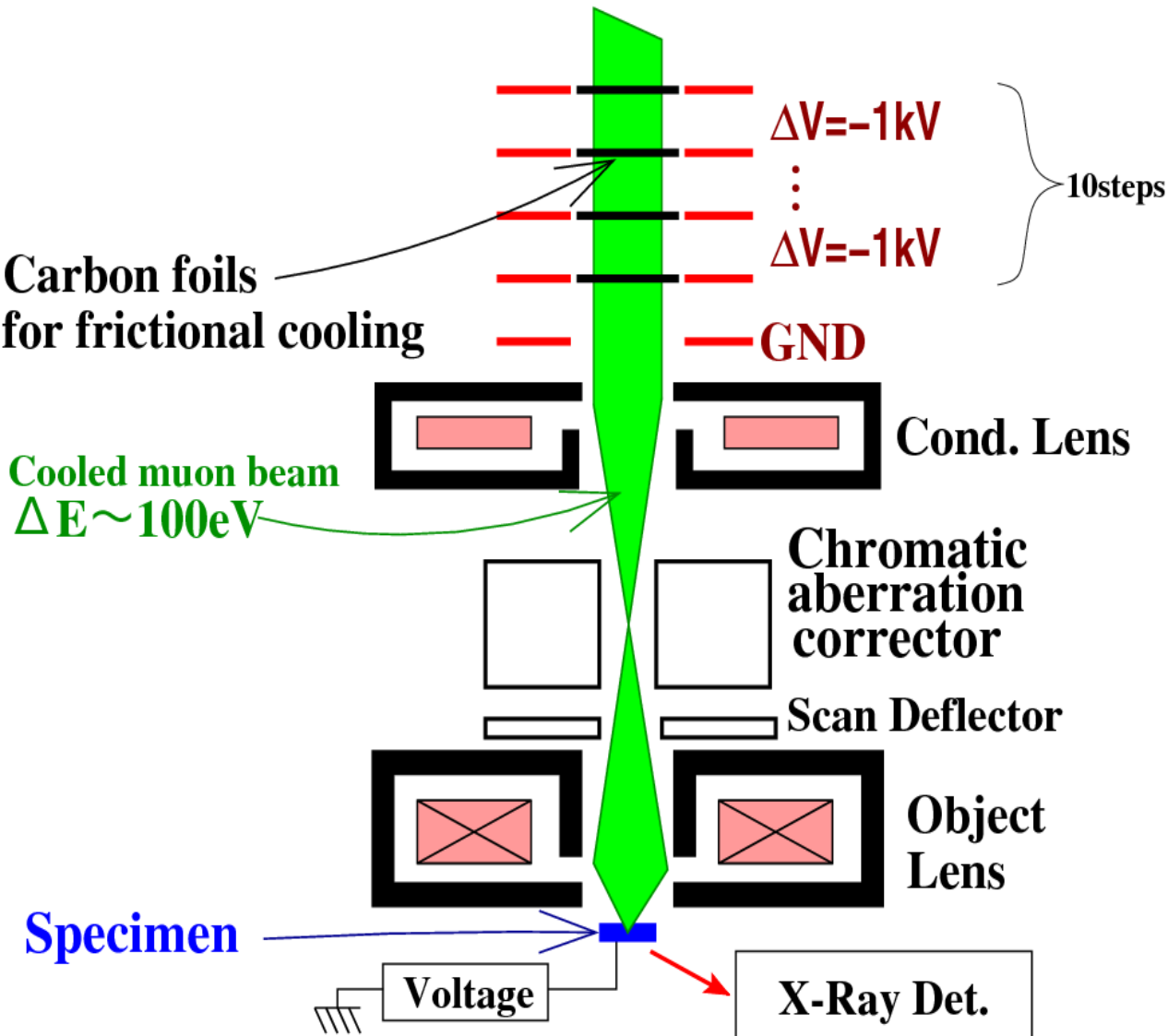
Simulation of Muon Collector



Simulation of Muon Collector



Parts of Cooler, Converge, Scan and Detection



- Frictional Cooling using carbon foils of 10nm thickness.
- Object Lens assisted by Chromatic Aberration Collector focuses beam into 10 μm diameter.
- XY-Scan, and retarding voltage scan.
- Detect X-ray Spectrum

3D mapping of Elements, Isotope and Chem.Props

Expected Performance

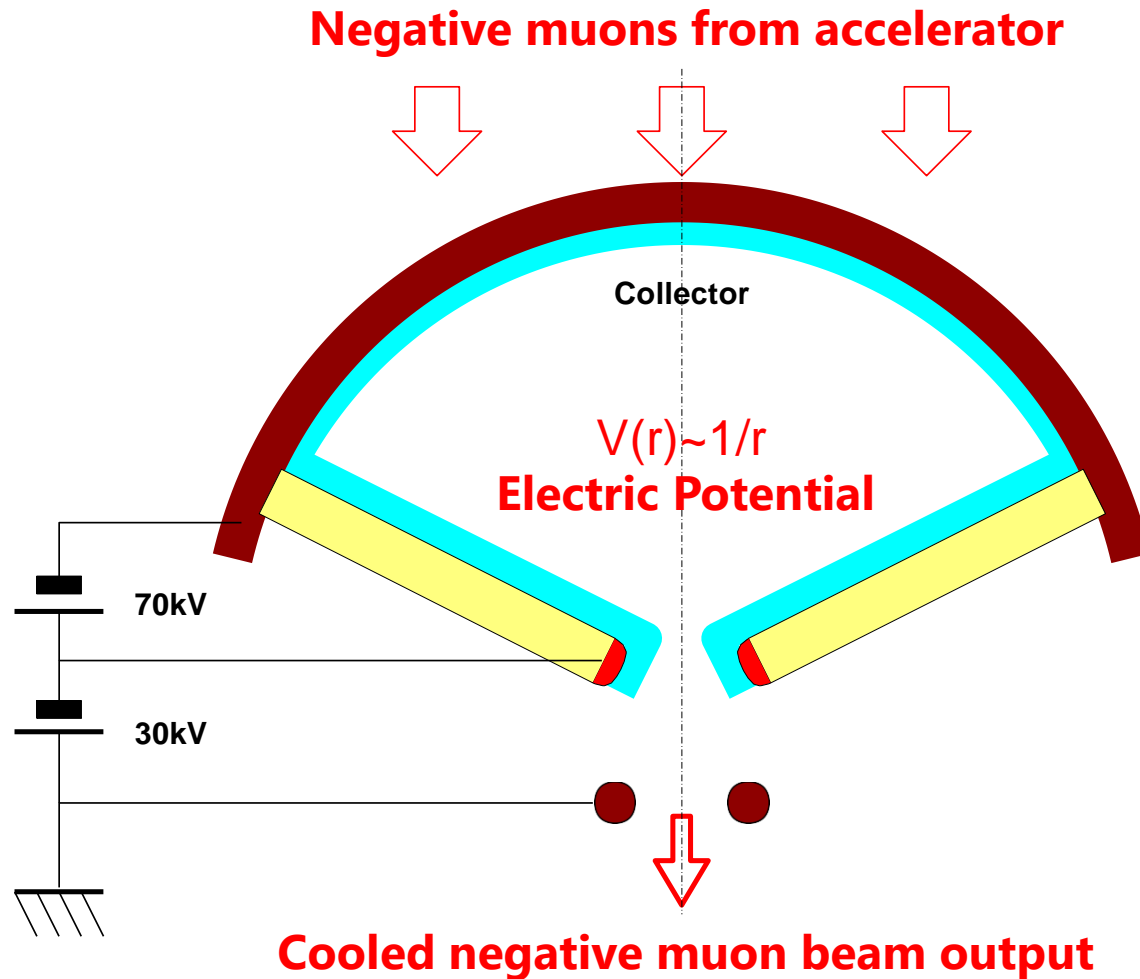
The S μ -M expected to have resolution <10 μ m, when Tritium is used. DD-fusion is less performance.

	DD-Fusion Only D	DT-Fusion using T
Re-emission rate of μ	2.0%	85.3%
Available # of μ CF cycle	Only 1 step	More than 10 steps
Diameter of extracted μ beam	10mm	<0.1mm
Diameter of focused μ beam	1mm	<10 μ m
Beam strength of μ	$\sim 1/\text{sec}$	$>30/\text{sec}$

$$\Rightarrow \text{Luminance Ratio (DT/DD)} = 100 \times 100 \times 30$$

Use of Tritium is essential.

Optimization of the neg μ collector

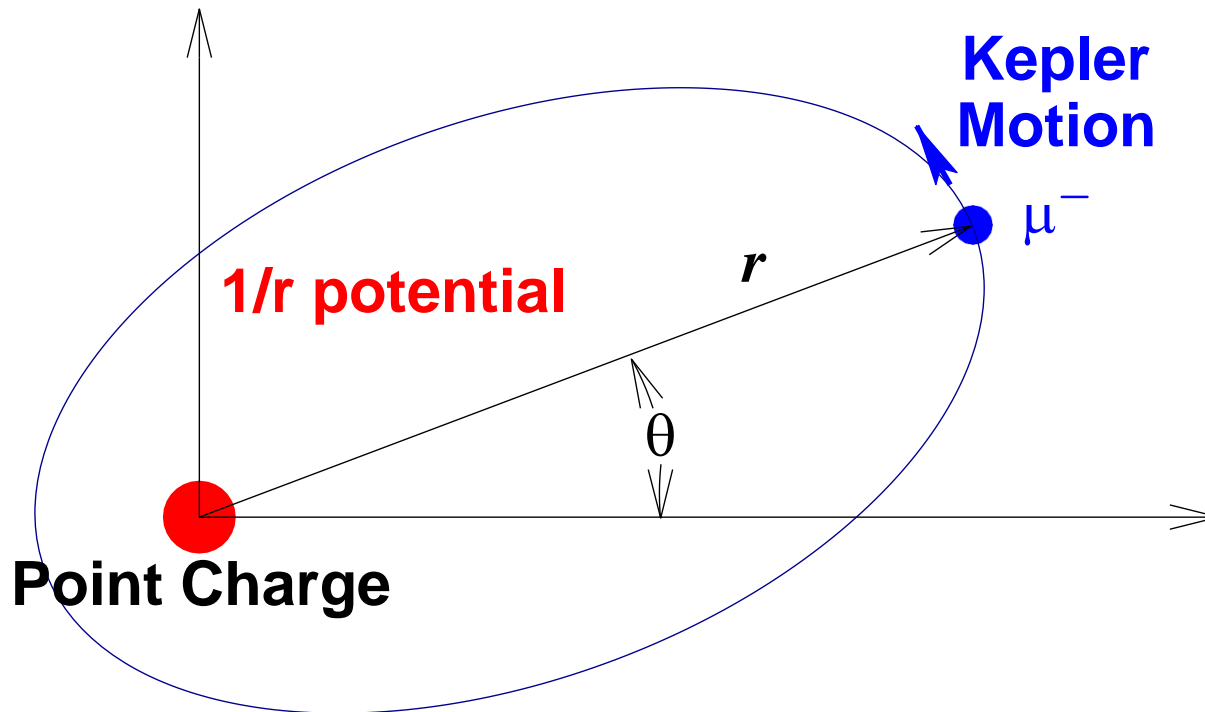


- We search **the most efficient design to collect μ^-** by electric potential $V(r) \sim 1/r$. For generalization, conical form of the collector is assumed.

Orbits under $(-1/r)$ potential : Kepler Motion

● Lagrangian:

$$L = \frac{m}{2} (\dot{r}^2 + r^2 \dot{\theta}^2) + V(r), \quad V(r) = -\frac{e V_S r_S}{r} \quad (1)$$



● Eq of Motion:

$$\ddot{r} = \frac{m^2}{l^2} \frac{1}{r^3} - \frac{eV_s r_s}{m} \frac{1}{r^2}, \quad (2)$$

constant : $l = mr^2\dot{\theta}$: angular momentum.

● General Solution (Eliptic curve) :

$$r = \frac{r_c}{1 + \varepsilon \cos(\theta + \alpha)}. \quad (3)$$

ε : eccentricity, α : phase, r_c : radius of circular-motion

$$r_c = \frac{l^2}{eV_s r_s m}. \quad (4)$$

- **A positive parameter depending on initial condition**
(initial position r_1 , projection angle β_1 , velocity v_1)
is introduced:

$$Q := \frac{\frac{1}{2} m v_1^2}{-V(r_1)} \quad (5)$$

When $Q < 1$, the orbit closes.

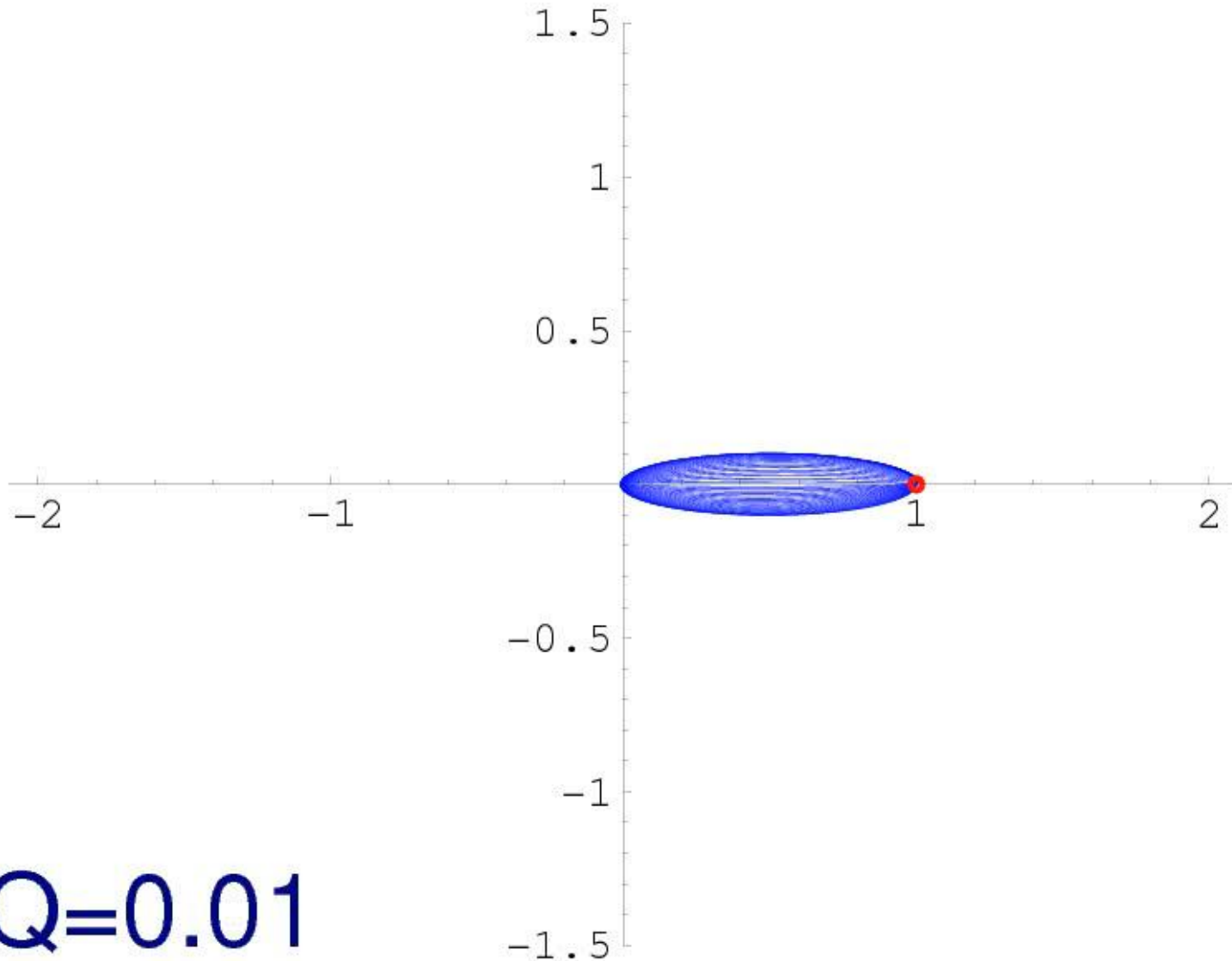
Q and β determine the motion :

$$\frac{r_c}{r_1} = 2Q \cos^2 \beta_1, \quad (6)$$

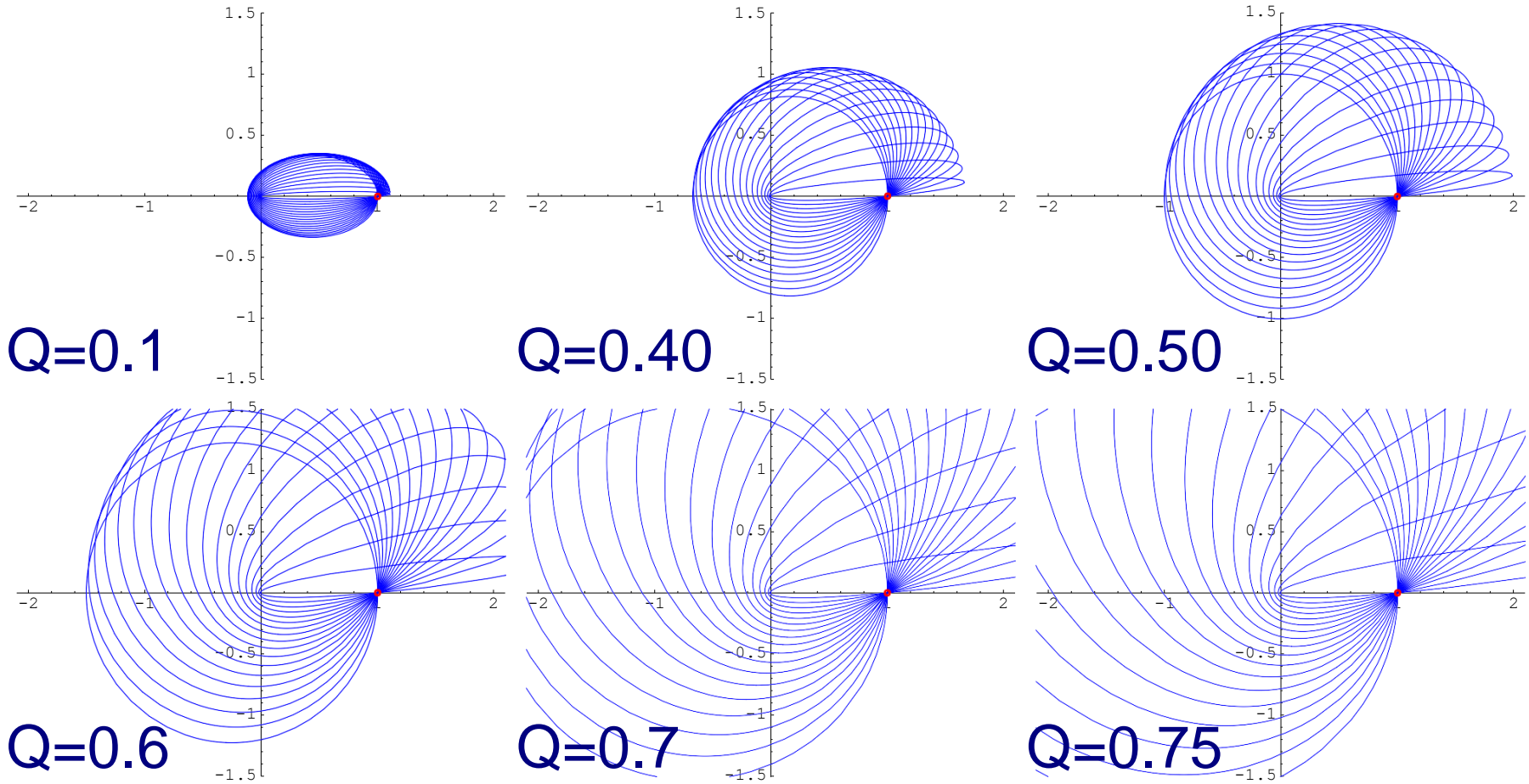
$$\varepsilon = \sqrt{1 + 4(Q - 1)Q \cos^2 \beta_1} \quad (7)$$

$$\alpha = \arg \left[\sin \beta_1 \cos \beta_1 + i \left(\cos^2 \beta_1 - \frac{1}{2Q} \right) \right] \quad (8)$$

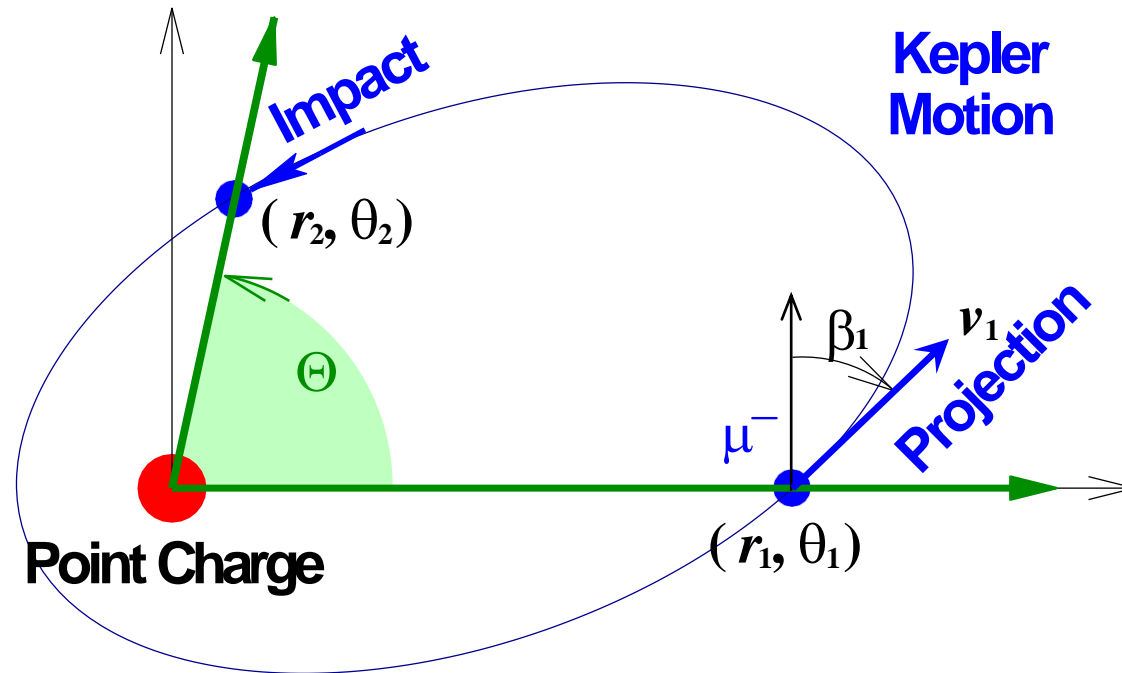
Orbits for projection angles β_1



Orbits for several Q



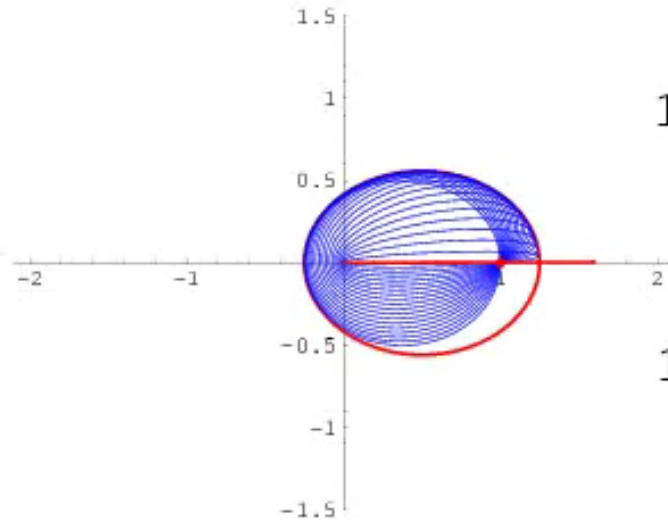
Impact point on counter side of fan



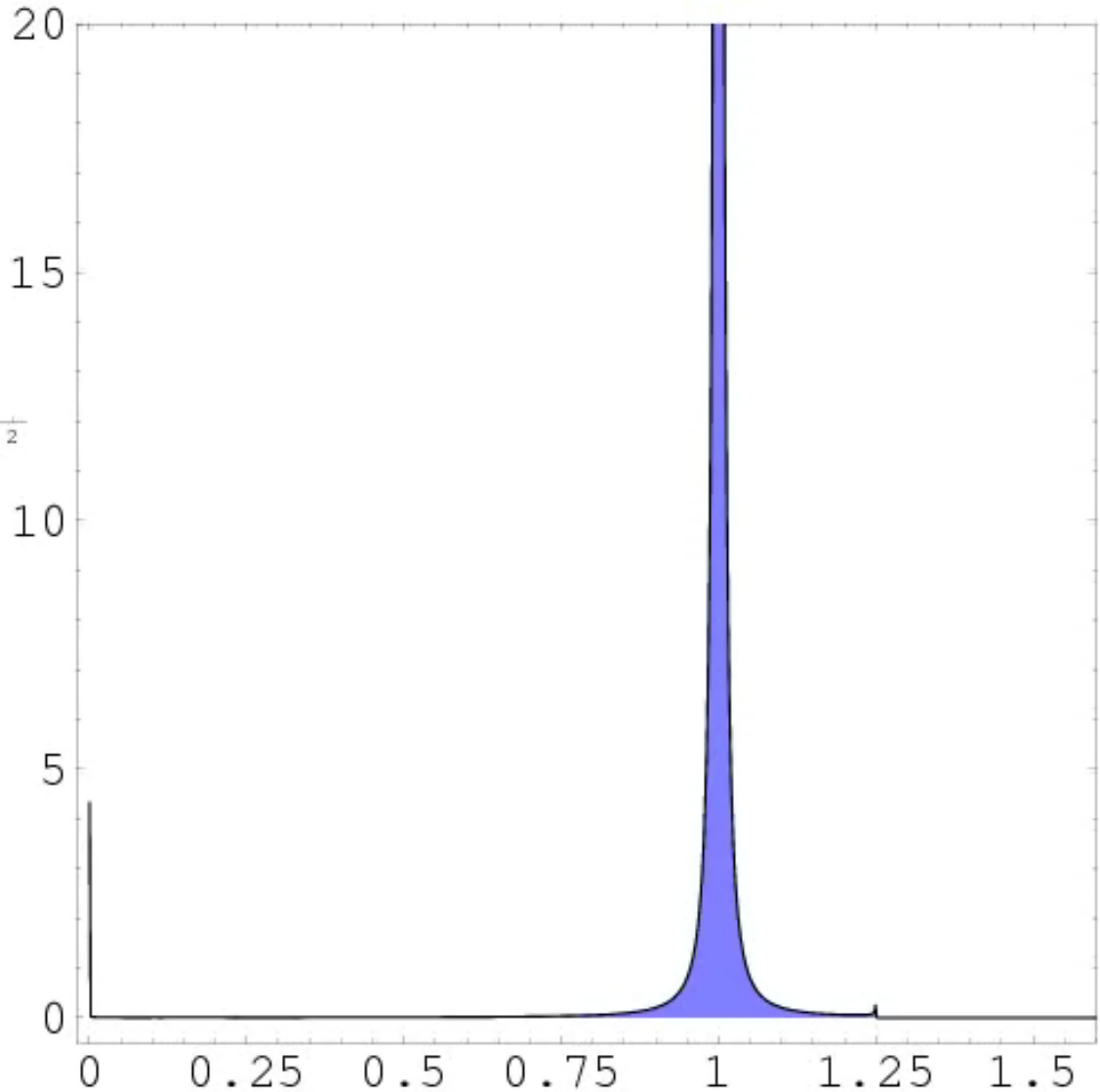
- By the motion from projection-point ($\theta_1 = 0$) to impact-point ($\theta_2 = \Theta$), radius changes as $r_1 \rightarrow r_2 = R \times r_1$, where R is mag/shrinking ratio.
- When distribution of projection-angle is fixed, the point splitting function (PSP) is obtained.

Distribution of Impact Points depending on Fan-angle

Projection-Angle-Distribution is assumed to be uniform.



$$Q = 0.2,$$
$$\Theta = 0.001\pi.$$



PSF is analytically derived for uniform-angle projection

$$\begin{aligned}
 n(R)^2 = & \left[+2R(\cos \Theta - R) \left\{ +\sqrt{1 + \cos \Theta}(-Q + R + \cos \Theta(Q - 1)R) \right. \right. \\
 & \left. \left. + \sqrt{2Q/R + \cos \Theta * (Q - 1)^2 + (Q - 1)(Q + 1)(\cos \Theta * R - 1)} \right. \right. \\
 & \left. \left. \right\} / (1 - 2 \cos \Theta R + R^2) \right. \\
 & \left. + \left\{ -2 * (\cos \Theta - 1) * R + Q(2 \cos \Theta R - 1) \right\} \sqrt{(1 + \cos \Theta)} \right. \\
 & \left. + \left\{ +((\cos \Theta - 1) + (\cos \Theta + 1)Q^2)(2 \cos \Theta R - 1) \right. \right. \\
 & \left. \left. + Q(-1/R + 5 \cos \Theta - 4 \cos \Theta^2 R) \right. \right. \\
 & \left. \left. \right\} / \sqrt{2Q/R + \cos \Theta(Q - 1)^2 + (Q - 1)(Q + 1)} \right]^2 \\
 & \times \left[+Q^2(1 - 2 \cos \Theta R + R^2)^2 / (1 - \cos \Theta) \right. \\
 & \left. - R^2 \left\{ +\sqrt{1 + \cos \Theta}(-Q + R + \cos \Theta(Q - 1)R) \right. \right. \\
 & \left. \left. + \sqrt{2Q/R + \cos \Theta(Q - 1)^2 + (Q - 1)(Q + 1)(\cos \Theta R - 1)} \right\}^2 \right]^{-2} \times \frac{1}{\pi} \quad (9)
 \end{aligned}$$

● PSF ($n(R)$) depending on fan-angle Θ :

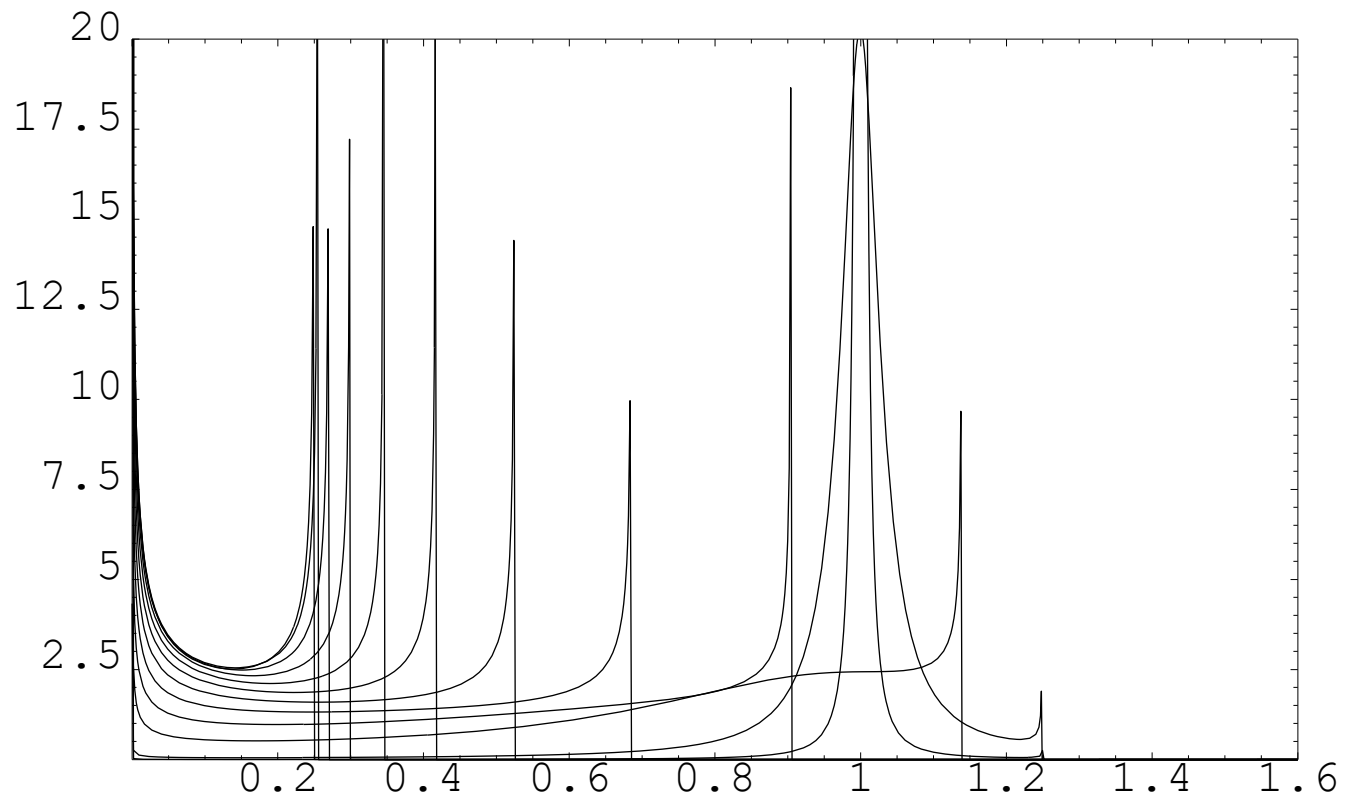


FIG: $Q = 0.2$, $\Theta/\pi = 0.001, 0.01, 0.1, 0.2, 0.3, \dots, 1.0$

● When $\Theta = \pi$, PSF becomes simple form :

$$n(R, Q) = \begin{cases} \frac{1}{\pi} \left[(1+R) \sqrt{(1-Q)R(R_{\text{sing}} - R)} \right]^{-1} & (R \leq R_{\text{sing}}) \\ 0 & (R > R_{\text{sing}}) \end{cases}$$

$$R_{\text{sing}} = Q/(1-Q)$$

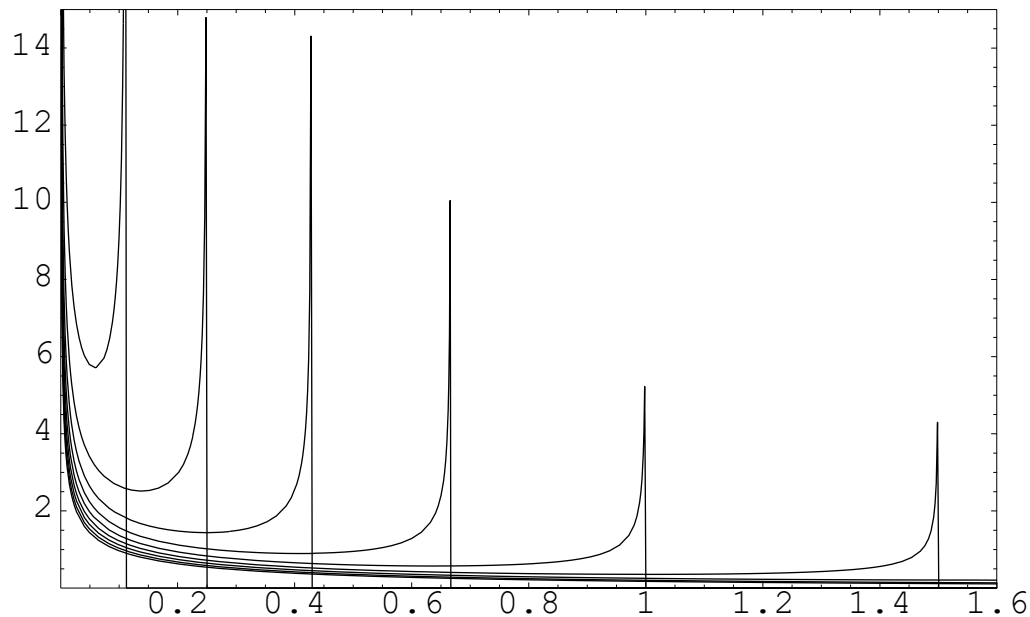


FIG: PSF for $Q = 0.1, 0.2, 0.3, 0.4, 0.5, 0.6, 0.7$, $\Theta = \pi$.

Average and deviation of mag-rate R

is defined by giving distribution of projection-angle $\rho(\beta)$:

$$\langle R \rangle := \int_{-\pi/2}^{\pi/2} d\beta \rho(\beta) R(Q, \Theta, \beta), \quad (10)$$

$$R^2 := \int_{-\pi/2}^{\pi/2} d\beta \rho(\beta) R^2(Q, \Theta, \beta), \quad (11)$$

$$\sigma^2 := R^2 - \langle R \rangle^2. \quad (12)$$

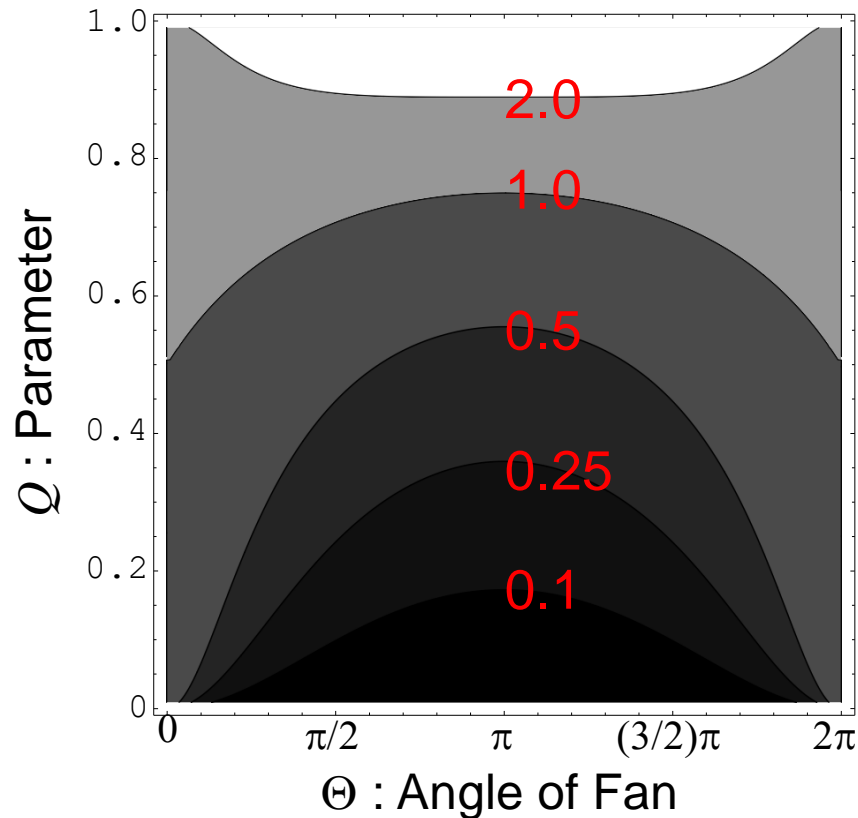
Here we will assume uniform distribution:

$$\rho(\beta) \sim \text{constant}$$

Average of Mag-rate R

$$\langle R \rangle = \cos \Theta + (Q + (Q - 1) \cos \Theta) \sqrt{\frac{\cos \Theta - 1}{Q^2 - 1 + (Q - 1)^2 \cos \Theta}},$$

Distribution of $\langle R \rangle$

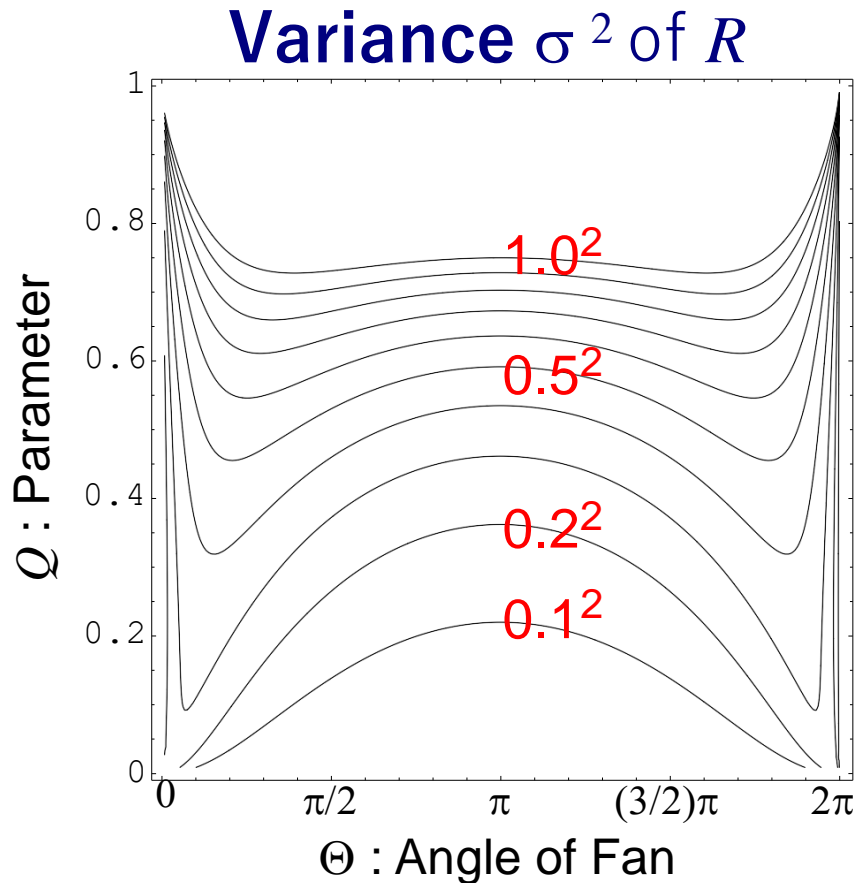


When $\langle R \rangle \leq 1$,
 $\langle R \rangle$ is minimized at $\Theta = \pi$.

Variance of mag-rate R

$$\langle R^2 \rangle = \cos 2\Theta + Q^2 \frac{-2Q \cos \Theta + \frac{1}{2}(3 + \cos 2\Theta)}{(-Q^2 + q^2)^{3/2}} - \frac{q \cos(2\Theta)}{(-Q^2 + q^2)^{1/2}}$$

(New parameter: $q := 1 + (Q - 1)\cos\Theta$.)



σ^2 is also minimize
when $\Theta = \pi$,
except for $Q \sim 0$

Optimized fan/cone-angle

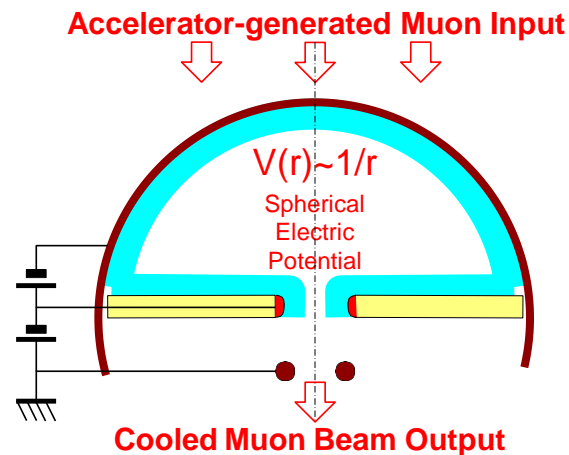
Theorem1:

For 2-dim, the fan-angle is optimized by $\Theta = \pi$.

Theorem2:

For 3-dim, the cone-angle is optimized by $\Theta = \pi$.
Disk Shape

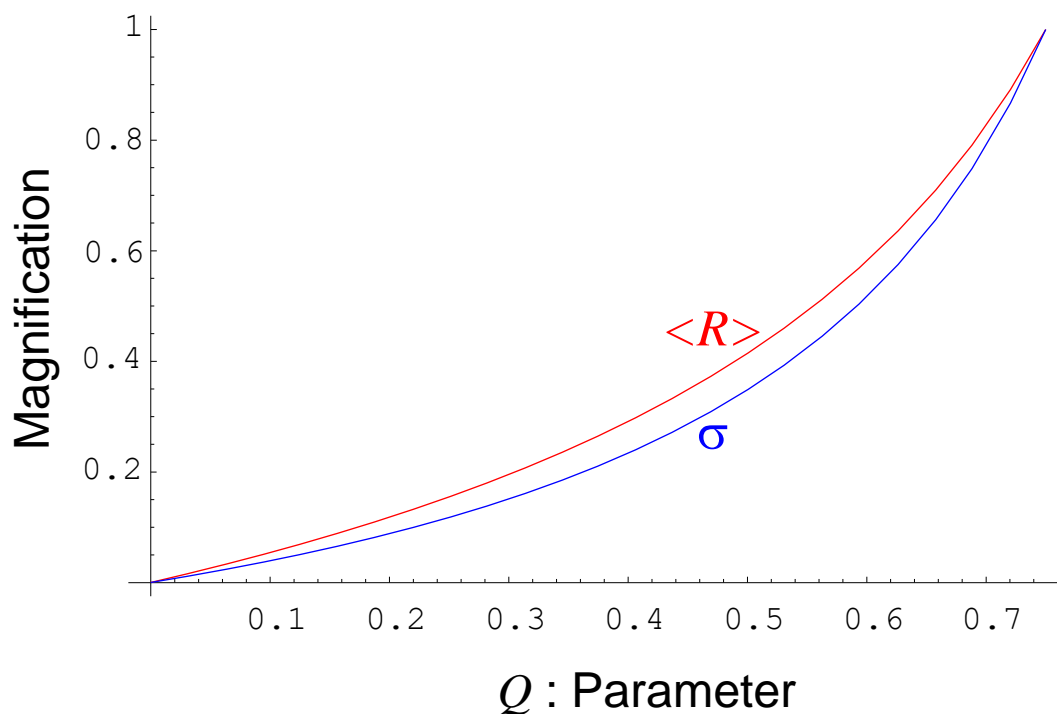
Shape of muon collector is optimized by disk-form rather than cone.



Ave. and Variance of Mag-rate of Disk Collector

$$\langle R \rangle = (1 - Q)^{-1/2} - 1, \quad (13)$$

$$\sqrt{\sigma^2} = \langle R \rangle \times \frac{1}{\sqrt{2}} (1 - Q)^{-1/4}. \quad (14)$$



Average $\langle R \rangle$ and variance $\sqrt{\sigma^2}$
of the magnification-rate R

Multistep cooling by Muon Collector

- Initial distribution $\eta_0(r)$ is given by accelerator
- By re-emission of muon by μ CF reaction, the distribution is developed as a generation:

$$\eta_0 \rightarrow \eta_1 \rightarrow \eta_2 \rightarrow \eta_3 \rightarrow \cdots \rightarrow \eta_n \rightarrow \cdots.$$

- Relation of generation :

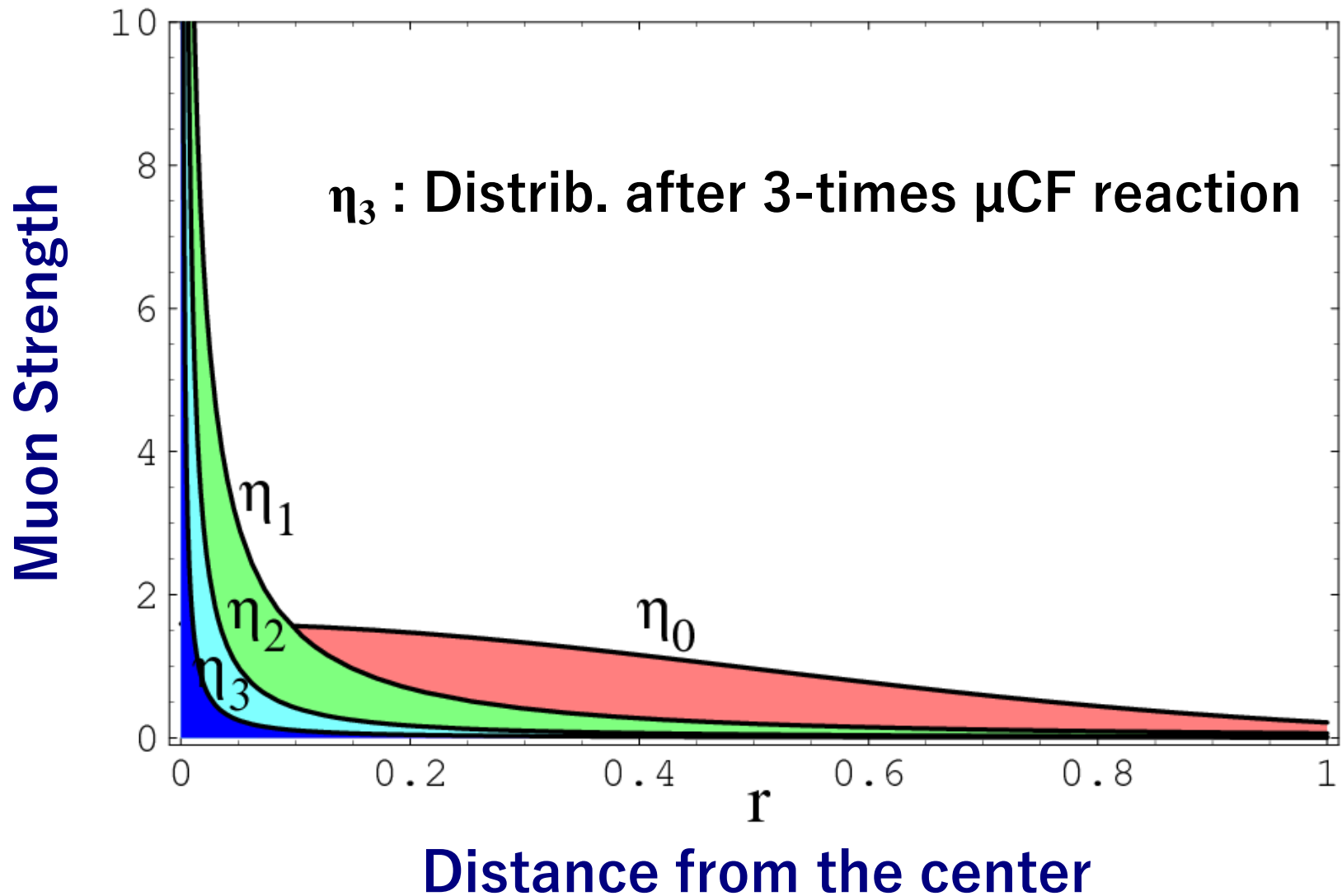
$$\eta_{n+1}(r) = \int_0^\infty d\tilde{r} K(r, \tilde{r}) \times \eta_n(\tilde{r}), \quad (15)$$

The integral-kernel depending on position r is derived from the PSP:

$$K(r, \tilde{r}) := \frac{1}{\tilde{r}} n \left[\frac{1}{\tilde{r}}, Q(\tilde{r}) \right]. \quad (16)$$

Evolution of the Generation

Gauss distribution $\sigma = 1/2$, $Q(\sigma) = 1$ is assumed as initial input.



Mag-Rate : Applying Volt. vs re-emission Energy

Re-emission energy ~ 2 keV

EV-ratio = Re-emission energy / Applying Voltage

	Generation of μ CF Reactions				
EV-ratio	0	1	2	3	4
10%	1	0.12	1.4×10^{-3}	2.0×10^{-7}	4.0×10^{-15}
50%	1	0.41	5.1×10^{-2}	6.6×10^{-4}	1.1×10^{-7}
60%	1	0.58	1.4×10^{-1}	6.2×10^{-3}	1.1×10^{-5}
70%	1	0.83	4.5×10^{-1}	9.2×10^{-2}	3.1×10^{-3}
75%	1	1	1	1	1

- We have assumed ideal potential $V(r) = C/r$.
- Mag rate becomes 1/1000 by applying 10kV with 4 \sim 5 μ CF generation.
- Possible generation is up to 10. (1-time makes 15% loss, 4-times make 50% loss)

Rate of the re-emission after slow muon impacts (Okutsu)

A: Re-emission rate from D or T

B: Possibility of releasing to front side

(1-B): Possibility of recapturing by D or T

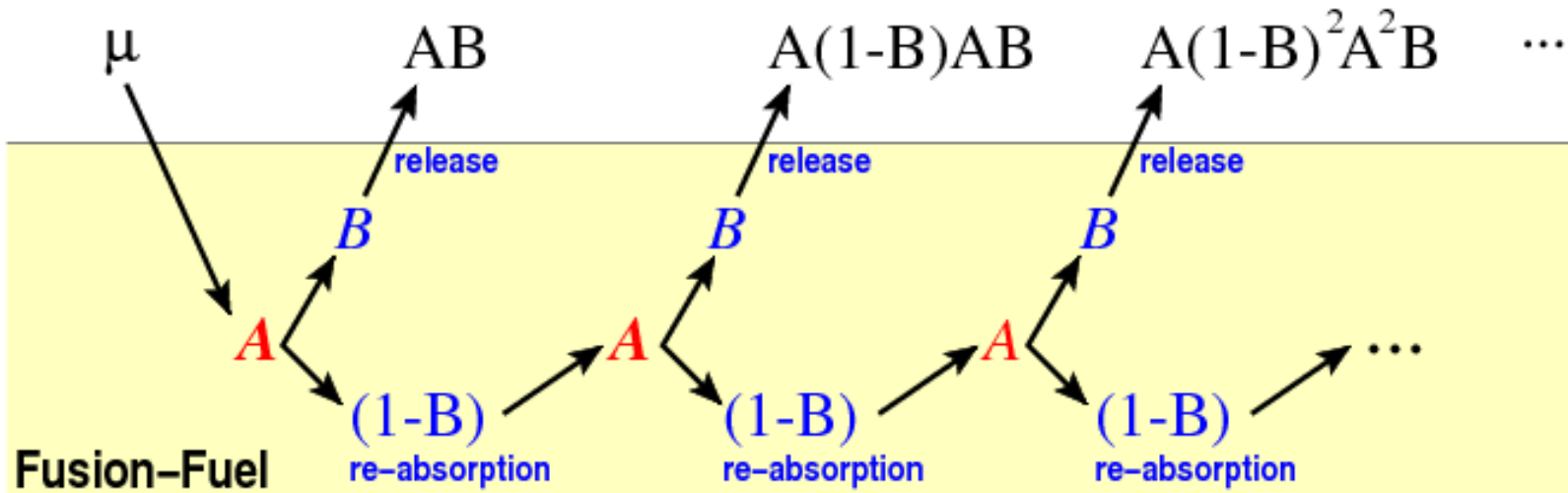
$$A_{DD}=0.16, \quad A_{DT}=0.98,$$

$$\sim 0.1,$$

$$\sim 0.9$$

(Calculated by impact $E=8V$, project $E=3keV$)

Sum of releasing probability by multiple μ CF reaction :



$$\begin{aligned}
 C &= AB + A(1-B)^1A^1B + A(1-B)^2A^2B + A(1-B)^3A^3B + \dots \\
 &= AB \sum_{n=0, \infty} (1-B)^n A^n \\
 &= AB / (1 - (1-B)A)
 \end{aligned}$$

DD-reaction : 2.0%

DT-reaction : 85.3%

... μ CF generation is only 1-time.

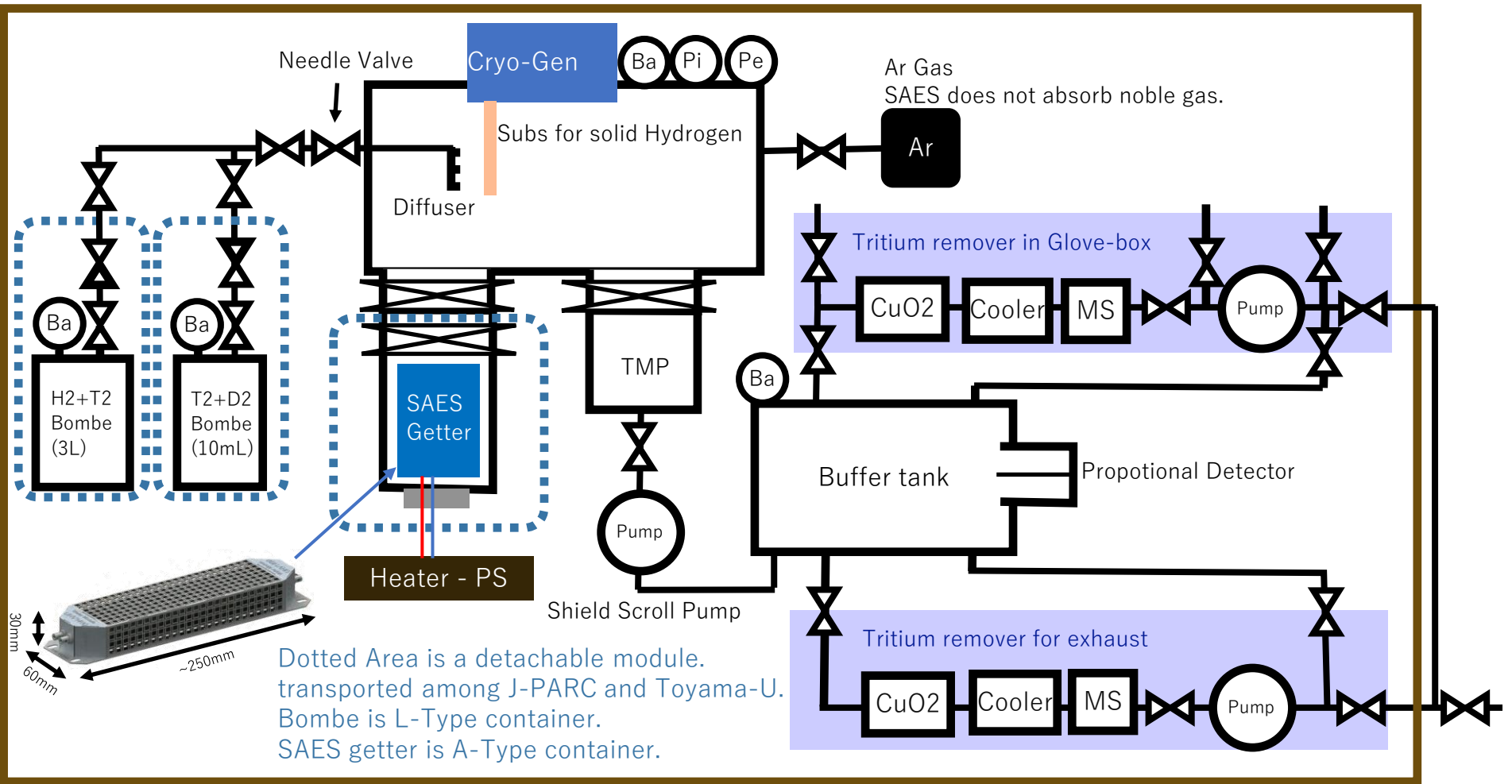
... μ CF generations can be 10-times.

Almost same result by Montecarlo Calculation.

Design of Tritium Handling

collaborating with Toyama U.

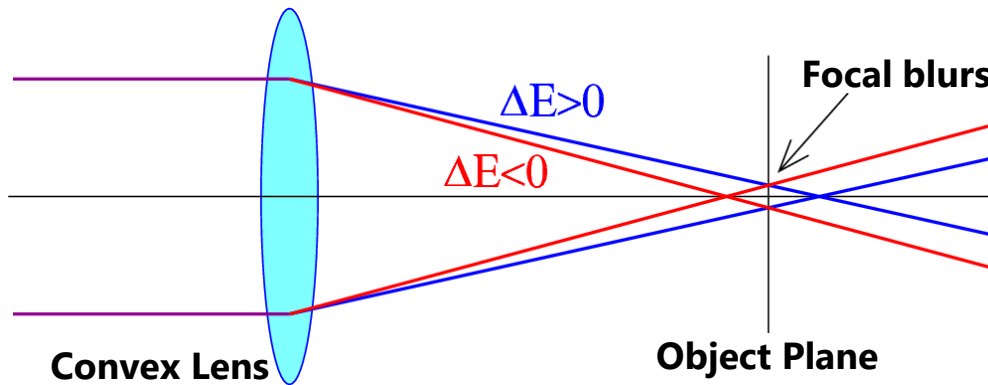
Glove-box



Designed by Hatano, Hara (Toyama U.), and Natori (KEK).

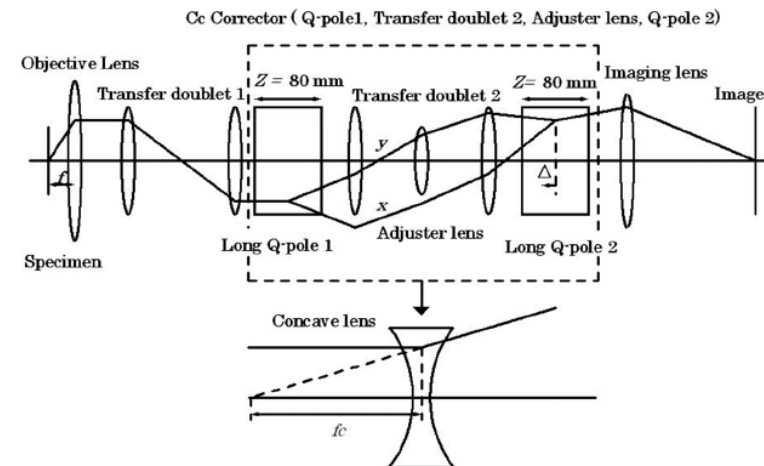
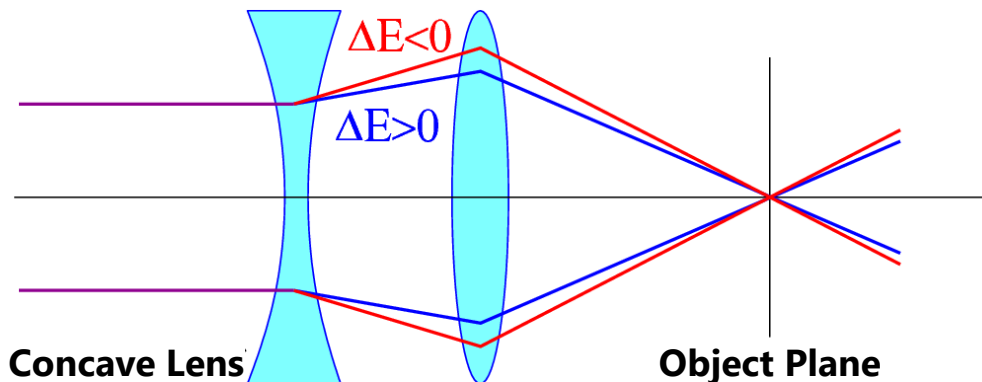
Beam Focusing by Aberration Corrector

- There is $\Delta E \sim 1$ keV even for beam-cooling.
- Chromatic aberration of conversion-lens blurs the focal point.



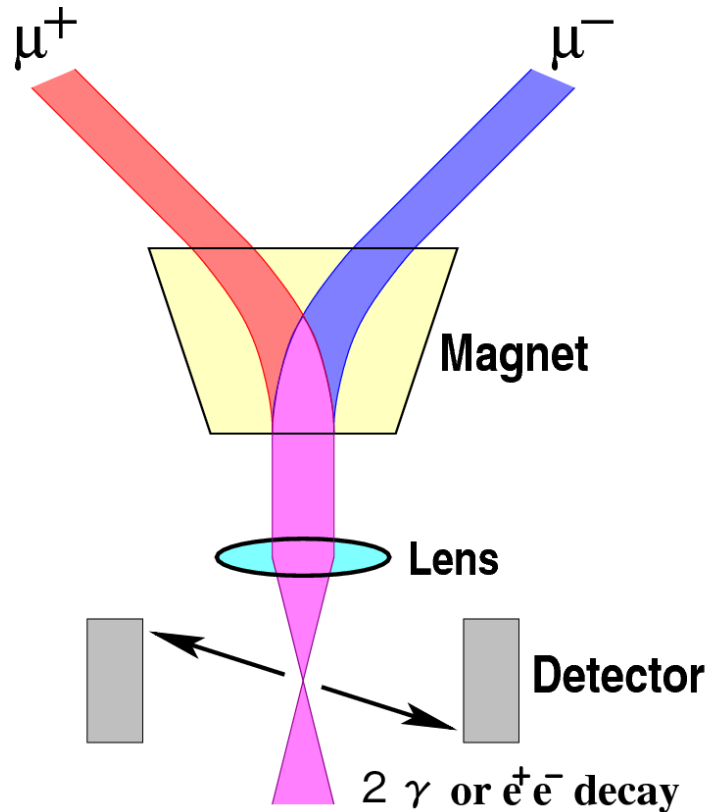
- Chromatic aberration corrector solves the problem.

Hosokawa Corrector



The other Applications of the Focused μ^-

● Generation of True Muonium $\mu^+ \mu^-$ and spectroscopy



● Beam source for Muon Collider ($\mu^+ \rightarrow \leftarrow \mu^-$)

● Soft-error evaluator for IC/LSI by focused μ^-